Design Study

of

Bolometric Scan Diagnostics

for JET[+)]

E.R.Müller

IPP III/56 January 1980

MAX-PLANCK-INSTITUT FÜR PLASMAPHYSIK

8046 GARCHING BEI MÜNCHEN

MAX-PLANCK-INSTITUT FÜR PLASMAPHYSIK

GARCHING BEI MÜNCHEN

Design Study of Bolometric Scan Diagnostics for JET[+)]

E.R.Müller

IPP III/56 January 1980

+) This work was done under contract No. B-GI-4o3 (article 14 of JET statutes)

Max-Planck-Institut für Plasmaphysik
EURATOM-Association, D-8046 Garching

Die nachstehende Arbeit wurde im Rahmen des Vertrages zwischen dem Max-Planck-Institut für Plasmaphysik und der Europäischen Atomgemeinschaft über die Zusammenarbeit auf dem Gebiete der Plasmaphysik durchgeführt.

Contents

1. Abstract

To establish a local energy balance and investigate plasma-wall interaction in JET, time and space resolved measurements of the total plasma radiation have to be made by means of a multichannel arrangement of bolometers. To calculate non-circular-shaped contours of the radiation emission coefficient in the plasma minor cross-section, a special arrangement of detectors has been designed: 4 bolometer arrays, each with 10 bolometers, are distributed around the poloidal circumference of JET. The bolometers of an array, which are mounted behind a common slit aperture, measure the radiation intensities integrated along different viewing chords. The measuring time resolution aimed at is 10 ms. Under the conditions of JET such measurements require arrays of reliable detectors which can be calibrated simultaneously and in-situ. The calibration data must have an accuracy and reproducibility of about $\pm$ 10 % and their time drift has to be within this range. Because JET will be operated with a D-T mixture the detectors have to be sufficiently insensitive to radiation damage. A gold resistor bolometer developed for ASDEX and a suitable electronic bridge circuit meet all these requirements. Absolute calibration is performed by means of a square-wave current pulse. Measurements with the bolometer in Pulsator have shown that an electronic bridge circuit using a reference bolometer shielded against VUV radiation largely reduces background signals, so that a detection limit in JET of better than 100 $\mu W/cm^2$ is to be expected. A preliminary design of the bolometer pinhole camera is presented. If offers the possibility of remote handling in the case of repair and maintenance. Further development work and future tests relating to this diagnostics are outlined.

2. Bolometric scan diagnostics in JET

2.1 The JET project

The JOINT EUROPEAN TORUS (JET) is a large tokamak with which it is intended to obtain and study a plasma in conditions and dimensions approaching those needed in a thermonuclear reactor. JET will be put into operation in Culham at the beginning of 1983. The project is described in Refs. /1/ and /2/ and all figures quoted in this report on bolometric scan diagnostics are taken from these two sources unless explicitly otherwise stated.

The main areas of work on JET are: the scaling of the plasma behaviour, plasma-wall interaction, plasma heating, and α-particle behaviour. The production of α-particles requires the use of tritium and will activate the apparatus. The guiding philosophy in designing JET was to retain the maximum operational flexibility illustrated by the variety of shapes, dimensions, modes of plasma operation and additional heating methods.

JET has a toroidal field of up to 3.5 T, the poloidal field can attain 0.6 T, the maximum plasma current is 3.2 MA, and, in the extended performance, with 25 MW of additional heating power, mean electron densities of 0.2 to 2 x 10^{14} cm^{-3} and mean plasma temperatures ($\bar{T}_e \simeq \bar{T}_i$) of 2 to 10 keV are expected. The geometric dimensions can be taken in part from Fig.8 and Table 2: the major radius is 2.96 m and the minor radii are 1.25 m (horizontal) and 2.10 m (vertical).

2.2 Objectives of the bolometric scan diagnostics

The aim of the bolometric scan diagnostics in JET is to make time and space resolved measurements of the total

plasma radiation with a multichannel arrangement of detectors. The bolometers have to determine quantitatively the total emission in the spectral range from 1 Å - which corresponds to an electron temperature of about 10 keV - to 2000 Å, and even to the infrared if the bolometer surface is blackened. Energy losses of the plasma due to neutral particles are also determined by the measurements, whereas charged particles, neutron radiation, high-energy X-radiation and γ-radiation should not contribute to the measuring signal. The measuring time resolution aimed at for JET is 1 ms to 10 ms, the latter being $\frac{1}{1000}$ of an assumed shot duration of 10s. The space resolution should be sufficient to yield contours of the radiation emission coefficient in the poloidal plasma cross-section from measurement of a large number of radiation intensities integrated along different chords through the poloidal plane: 20 parallel viewing chords per plasma minor cross-section normally meet this requirement, but because the JET plasma is of non-circular shape 20 additional chords at an angle of 90° to the first are needed. The absolute and relative accuracy of the measurement should be about 5 %.

In addition to the bolometer arrays in JET, there should be so-called single bolometers which view the whole plasma minor cross-section and are distributed around the toroidal circumference of JET. By means of these we can test the toroidal symmetry of the plasma radiation, normalize the scan measurements and reach a higher time resolution because the signals of these detectors will be larger than those of the bolometers in the arrays.

The radiation losses measured by bolometers are mainly caused by line radiation and bremsstrahlung of impurities in the plasma, and, in present-day tokamaks, represent one of the most important energy loss channels determining the energy confinement time τ_E /3,4/. Measurement

of radiation contours with bolometers is therefore an essential element for establishing a detailed and local energy balance. From a computer analysis of measured profiles of $T_e(r)$, $T_i(r)$, $n_e(r)$ and total radiation $P_{rad}(r)$ we get the radiation-corrected energy confinement time of the electrons as a function of the radius $\tau_{E,e}(r)$ and, furthermore, profiles of the electron heat conduction coefficient $\chi_e(r)$ /5/.

The radiation profile has a decisive influence on the profiles of other plasma parameters, e.g. $T_e(r)$ and $j(r)$, which, in turn, strongly influence the generation and transport of radiation emitting impurities. Thus, to understand plasma parameter profiles, e.g. hollow temperature profiles and the physical processes underlying them, a knowledge of the radiation distribution is necessary /1,2,6,7/.

The theory also predicts how the parameters $\tau_E, \tau_{Ee}, \chi_e$ describing the energy confinement scale with plasma parameters such as T_e, n_e /4,8/. The physical models on which the scaling laws are based can be tested by means of the above experimental determination of $\tau_{E,e}(r)$, $\chi_e(r)$.

Time and space correlation of bolometric results with spectroscopic data allows the main types and sources of impurities to be identified and suggests ways of reducing the plasma impurity content. Observation of radiation as an indicator of impurities permits us to study effects of plasma-wall interaction and the efficiency of such means of lowering the impurity concentration as gas puffing, Ti-gettering, use of a divertor /4,9,10/.

By means of bolometers it is possible to measure transient phenomena on a time scale of ms: During MHD or microinstability processes such as the internal disruption the radiation emission coefficient as a function of the radius and time $\epsilon(r,t)$ undergoes rapid changes /11/.

2.3 Further requirements to be met by the multichannel bolometer diagnostics and consequences

The environmental conditions under which the bolometer has to work reliably in JET are extreme: the vessel to which the bolometer is attached is baked to 500 °C; the bolometer system has to meet ultra-high-vacuum (UHV) requirements; neutron and γ-radiation caused during D-T operation of JET activates the whole machine and makes remote handling necessary when repairing or replacing bolometers and can even cause radiation damage of detectors and electronic components if they are not properly designed.

During a shot temperature drifts of the vessel, heat loads due to penetrating neutrons and high-energy γ-radiation and fluctuating magnetic fields cause background signals which have to be eliminated by a compensation method, i.e. the background signal of a second bolometer shielded against VUV radiation, the so-called reference bolometer, is subtracted from the signal of the (unshielded) bolometer by means of an electronic bridge circuit. The reference bolometer has to be located immediately next to its respective bolometer.

To obtain the maximum possible information about a non-circular-shaped plasma from every single shot, i.e. to get contours of the radiation emission coefficient even if the shots are not reproducible, it is absolutely necessary that several bolometer arrays be placed in the poloidal plane around the plasma.

With a multichannel arrangement of detectors and electronic bridges under the boundary conditions stated, the bolometers must meet specific requirements, which need not be imposed if, for example, a scan were to be made from shot to shot with a single bolometer. The type of detector, the relevant electronics, the calibration procedure and the data evaluation method are not independent of each other but have a

mutual bearing. We need bolometers which are both very sensitive to VUV radiation and very robust, reliable and resistant to radiation damage. Their calibration data should be reproducible and should not drift with time. It should be possible to calibrate them simultaneously in-situ, and to perform the calibration procedure automatically in a short time and as often as required. The design of the bolometer has to satisfy the requirements concerning the vacuum and temperature ranges and should allow replacement of bolometers by remote handling.

The available detectors, a thermopile detector /12/, a semiconducting bolometer /13/, a thermistor bolometer /14/ and a pyroelectric detector /10/ (bolometers applied to tokamaks are reviewed in /15/), do not meet all the requirements for JET. In general, they are not reliable enough, are sensitive to radiation damage and cannot be calibrated in-situ or their calibration data are not reproducible and drift with time. A metal resistor bolometer and a method using infrared (IR) observation of a preheated metal foil /17/ are suitable in principle. The metal resistor bolometer is the only one of the two types which has both been successfully tested in a tokamak and used to design a pinhole camera, to be put into operation in ASDEX during 1980. In view of the complexity of the measuring problem in JET we consider it indispensable that during the design phase of JET it should be possible to enlist the experience gained meanwhile with a very similar multichannel measuring device in one of the existing tokamaks. For this reason we concentrate in this report on the metal resistor bolometer, the other types of detectors being treated briefly.

3. Detectors

3.1 Metal resistor bolometer

Figure 1 shows schematically the design of the existing metal resistor bolometer, which was developed for ASDEX and will be described in detail in /16/. A 1 cm^2 large, quadratic, 4 μm thick gold foil almost totally absorbs the VUV radiation from about 10 Å to 2000 Å (/18,19,20/ and Figs. 3,4). The subsequent temperature rise of the foil causes a change of resistance in a 5 kΩ gold resistance layer which is separated from the gold absorber foil by 7.5 μm thick capton foil. This dielectric is thin enough to enable heat transfer in less than 100 μs but is sufficiently thick to make the bolometer extremely robust. The capton surface is covered almost completely and uniformly with a gold resistor in the form of a meander. All the bolometers have a resistance of 5 kΩ $\pm$ 10 %, this rather high resistance value being reached by applying photolithographic techniques in the manufacturing process.

The foil is mounted between two SS rings which are bevelled to reduce the aperture effect of the mounting rings as far as possible. The meander runs into two contact surfaces on which two gold-plated contact pins press. As a rule, this contact is made just once. Thereafter, the foil mounting rings and bolometer holder are left screwed together and constitute a module which can readily be replaced by means of two mechanically stable plugs, even in the case of remote handling (Fig.2).

To extend the light absorption of the bolometer to the infrared, it would be necessary to blacken the gold absorber foil. We propose that this not be done in the case of the bolometer array. A layer of 'black gold' /21/ makes the bolometers mechanically sensitive and they are no longer reproducible in their technical und calibration data. In Sec. 4 we shall

show that we neglect radiation cooling in the evaluation formulae for the bolometer measurements and this assumption would no longer be true if we were to blacken the foil. Without a 'black gold' layer the VUV radiation is absorbed up to 2000 Å (Fig.4), and we should consider that nearly all of the JET radiation will be emitted below 2000 Å. To compare the results obtained with blackened and unblackened detectors, we can blacken one of the single bolometers distributed around the torus (Sec.8.2).

The first part of Table 1 lists the technical and calibration data of the existing bolometer. The calibration procedures and the meaning of the calibration data such as cooling time constant τ_c, heat capacity C, heat resistance z, temperature coefficient α, and response r are treated in Secs.4 and 4.1 of this report, while the detection limit is treated in Sec.5.2. One has to distinguish between the response time, which is characteristic of heat conduction through the capton foil, the cooling time τ_c, describing the cooling-down process of the bolometer foil by heat conduction to the mounting rings, and the measuring time constant, which strongly depends on the machine-specific background signals and electronic filter characteristics.

In the case of JET we have to increase the thickness of the gold absorber foil to about 15 µm to enlarge the absorbed spectrum range down to 1 Å. This will shift some of the calibration data to new values which are calculated by formulae (6,7) of Sec.4 and listed in the second part of Table 1.

Table 1: Bolometer data

I) Pulsator/ASDEX bolometer

- measuring time resolution	ASDEX: 1 ms (target set) Pulsator: 10 ms
- response time	100 µs
- cooling time τ_c	173 ms
- heat capacity C	2.0 mJ/^{o}C
- heat resistance z	0.09 ^{o}C/mW
- electrical resistance	5 kΩ
- temperature coefficient α	0.26 % $^{o}C^{-1}$
- response r (with a bolometer current of I_B=2 mA)	2.21 mV/mW or 26 mV/^{o}C
- detection limit in Pulsator:	
a) signal proportional to absorbed radiation power	270 µW or 1.7 x 10^{-2} ^{o}C in steady state
b) signal proportional to temperature rise of the bolometer	35 µW stationary power or 6.5 µJ or 3.9 x 10^{-3} ^{o}C

II) Extrapolation of JET bolometer

- measuring time resolution	10 ms (target set)
- heat capacity C	4.5 mJ/^{o}C
- heat resistance z	0.04 ^{o}C/mW
- response r (I_B=2 mA)	1.0 mV/mW or 26 mV/^{o}C

The advantages of the metal resistor bolometer are as follows: The capton foil as a substrate for the deposited metal films lends the bolometer extreme mechanical stability and allows both high measuring voltages with a sufficient safety margin of 280 kV/mm to the breakdown voltage of the capton foil and baking of the bolometer to more than 200 °C.[x]) The metal resistance shows a linear temperature response and nearly no drift with time, just as all the calibration data (Table 1) are reproducible and stable in time within a limit of ± 10 %. This limit includes different batches of bolometer foils and calibration data of the bolometers which were obtained both before and after use of the bolometers in Pulsator. Because of the uniform coating of the bolometer foil with the gold resistor, absolute in-situ calibration is possible by depositing quantitatively defined ohmic heating power on the foil surface by means of the measuring current, thus simulating irradiation of the bolometer. The detection limit of the bolometer system is comparable with or even better than those of other detectors. The fact that the bolometer detector head (mounting rings plus contacts) is designed as a reproducible module gives us the possibility of compensating background signals by an electronic bridge circuit with a reference bolometer and, secondly, of performing remote handling operations on the activated tokamak.

All these properties were confirmed in long test series in the laboratory and in Pulsator, especially the extremely high operational reliability of the bolometer and stability of its calibration data. The materials used for constructing the bolometer are insensitive to radiation damage if we limit ourselves to 20,000 JET discharges with D-T mixture. More on this rather important subject is presented in Secs. 9 and 9.1.

---

[x]) Capton can be used in the temperature range up to 400 °C. In laboratory experiments until now we have only baked the bolometer to 200 °C, no damage being thereby incurred. Further experiments should be made with higher temperatures to determine the effect on calibration data and the destruction limit of the bolometer.

To summarize, it can be stated that this bolometer type meets all of the requirements listed in detail in Secs. 2.2 and 2.3. During the design work for JET test series can be conducted for the purpose of finding resistor materials with a temperature coefficient higher than that of gold. The problem is that the material will have to be just as suitable for the manufacturing process as gold, and that it will have to endow the bolometer with the same excellent properties in the way of stability of the calibration data. Experiments with nickel, for instance, were unsuccessfull.

3.2 Other detectors

I) Semiconductor and thermistor bolometers

There exist bolometers which use a semiconducting resistor layer /13/ or a commercially available thermistor /14/ to measure the temperature rise of the bolometer foil. In the semiconductor bolometer the Ge resistor layer is separated by a MgO layer from the metal foil absorbing the VUV radiation. In the thermistor bolometer the small thermistor plate (0.5 mm x 0.5 mm x 40 μm) is directly attached to the absorber foil. Both bolometers have the advantage of having a relatively high temperature coefficient α. But they are extremely sensitive to radiation damage (Sec.9.2) because during a plasma shot high-energy neutron and γ-radiation cause lattice defects as well as ionization in the resistor layer, both effects having an enormous influence on the electrical resistance of these materials. In the thermistor bolometer this suspicion was confirmed by a fission reactor test /22/: A radiation dose of 10^7 rad caused an irreversible change in detector response by a factor of 2. The bolometer types described in this section are thus unsuitable for measurements in JET.

The Ge bolometer is, moreover, sensitive to mechanical damage; electric breakdown of its MgO dielectric cannot be reliably prevented, and the use of bridge electronics which largely reduces background signals (described in Secs. 5.1 and 5.3) is not readily possible for a whole array of bolometers of this kind because the technical and calibration data of this detector are not reproducible enough and their drift with time is too large. Applying such a bridge electronics to the gold resistor bolometer, we can neutralize the disadvantage of the smaller temperature coefficient of metals and reach values of the detection limit comparable with those of semiconductor and thermistor bolometers (Sec. 5.2).

II) Thermopiles

In our opinion, thermopiles, described in Ref. /12/, offer no advantages over bolometers.

The absence of a measuring current deprives one of the possibility of using it to calibrate the detector in-situ and, secondly, the response, expressed in units of $V/^{o}C$, is at least one order of magnitude lower than that of bolometers.

III) Pyroelectric detectors /10/

The electric polarization of a ferroelectric crystal such as $LiTaO_3$ is a function of temperature and can be used to measure the temperature of the detector foil. The detector supplies a current which is proportional to the temperature change with respect to time. Because this current is very small, a current amplifier has to be placed immediately next to the detector inside the vacuum vessel of the tokamak. Severe difficulties are already being encountered in interpreting the measuring results gained with these detectors in the existing tokamaks DITE and TFR /23/. One of the reasons is very probably radiation damage during runaway discharges. Further problems are the falsification of the signal due to the electrons produced by secondary emission and the enormous time drift of the calibration data.

IV) Thermographic method

In this measuring method the temperature of a metal foil absorbing the VUV radiation is determined by measuring the infrared (IR) emission from the foil by means of an IR optical detection system /17/. The tantalum foil with an area of 3 mm x 60 mm and a thickness of 6 μ is preheated to 100 ^{o}C with a DC current of about 0.4 A which is stabilized to 10^{-4}. The IR radiation emitted from the blackened foil surface is transmitted to an InSb detector cooled with liquid N_2 by IR optics. The radiation is chopped (400 c/s) and the signal can thus be detected by lock-in technique. Absolute calibration is done in-situ by applying a current pulse to the metal foil ($R \simeq 0.4\Omega$).

The attraction of this method is obviously that the sensitive detector can be remote from the torus and the measuring signal is decoupled optically.

But this measuring principle also entails several problems. On the one hand, preheating of the foil with a high current is absolutely necessary because this improves the signal-to-noise ratio (SNR) by a factor of 8 to make the method competitive with others; on the other, the current in connection with the magnetic field of the tokamak exerts such strong forces on the foil that the tearing limit of the material is reached, thus exposing it to damage. For this reason a gold foil, for instance, cannot be applied. The procedure of optically transmitting the signal of interest avoids electrical pickup by way of the cables. But because the optical path has to be sufficiently long (see below) small mechanical vibrations can cause large interference signals and the advantage of optical decoupling can thereby be more than just neutralized. This, at any rate, was the practical experience gained in TFR during the last few years.

Another difficulty is the extremely high sensitivity of an InSb detector (InSb belongs to the group of III - V compounds) to radiation damage. This detector thus has to be located far from the torus - implying very large optical path lengths - and very efficiently shielded against radiation. The whole system has a nonlinear response curve, and so the calibration procedure is more complicated than that described in Sec.4.1 and the calibration data depend on the working point on the response curve. In the evaluation formula - corresponding to eq.(1) of Sec.4. - cooling of the foil strip due to heat conduction is neglected in TFR, only radiation cooling being taken into account. This would not be justified in the case of JET because of its long shot durations and it should be borne in mind that the presence of both terms describing cooling processes in the differential equation considerably complicates the evaluation problem. Further specific problems of this sort of radiation detection are that the preheating current has to be kept sufficiently constant, otherwise this falsifies the signal, that a compensation method has to eliminate the portion of the signal due to background radiation, that the electrical resistance of the metal foil has to be known with sufficient accuracy, that an improperly designed chopper may introduce additional interference signals, and that in building an array of foils the blackening of the various foils should not be too different.

The detection limit of such a thermographic system was theoretically estimated at about 10^{-2} °C - using rather optimistic assumptions such as that the noise would be only 5 times as large as the noise due to photon statistics. (This value has to be compared with data of Tables 1 and 3.) Experimental results relating to the detection limit and the accuracy, reproducibility and drift of calibration data are not yet available from TFR (status of mid-January 1980). For

this reason and because a compensation method of the kind specified in Sec.2.2 has not yet been provided for TFR, let alone a multichannel arrangement of detectors, we should like to propose that further developments at Fontenay be awaited first before reconsidering the usefulness of the thermographic technique for JET.

An alternative possibility of scanning the temperature profile along a one-dimensional array of metal foils would be to operate an infrared scanning camera (e.g. type AGA THV 780) in the line scan mode. The difficulties described above, however, still persist. The detection limit of such a camera scanning with 2.500 c/s amounts to 0.2 ^{o}C and one has to average over at least 100 scans to obtain a detection limit comparable with that of other detectors, but then the time resolution would no longer be good enough. A second difficulty inherent in this technique is that one first has to digitize (and store) the infrared data and only then can they be differentiated with respect to time to solve eq.(1) of Sec.4. This makes the method even more insensitive.

4. Introduction to theory of the bolometer

If a radiation power P is uniformly incident on an area A of a bolometer foil with a thickness d, the time behaviour of the temperature of the foil is governed by the differential equation

$$\frac{P/A}{(c\varrho d)} = \frac{d}{dt} T + \frac{1}{\tau_c} T \qquad \text{or} \qquad (1)$$

$$P = C \frac{d}{dt} T + \frac{1}{z} T \qquad (2)$$

if we use

$$\tau_c = C \times z \qquad (3)$$

where T is the temperature rise of the foil above an equilibrium temperature and C its thermal capacity; τ_c, the cooling time constant, is a measure of the heat losses due to heat conduction from the gold absorber foil to the SS mounting rings (Sec.3.1); z is defined by eqs.(3) and (10) and is called the heat resistance of the bolometer; c and ϱ are the specific heat and the density of the material. Because the temperature equalization over the thickness of the foil can be assumed as instantaneous (< 100 µs), c and ϱ denote values averaged over the three layers of the bolometer and C is also valid for the whole foil.

Equation (1) states that if we measure the time dependence of T we are able to determine the radiation emitted from the plasma at any time, irrespective of how large τ_c is, provided, of course, that the assumptions underlying eq.(1) are justified.

The main assumption is to neglect the dependence of T on the space coordinates, i.e. one acts as if the foil had a uniform temperature over the whole area. This would be a

really good approximation if, for example, radiation cooling dominated the heat losses of the foil. In actual fact, however, heat conduction losses largely predominate if the bolometer surface is not blackened. In this case eq.(1) still describes correctly the time behaviour of T at every point of the foil if the temperature profile across the foil can be expressed by a cosine function. All our tests in the laboratory showed (see below) that the time evolution of the temperature T averaged over the foil surface obeys eq.(1) to a sufficient degree of accuracy. In Ref./16/ we shall nevertheless present the complete theory and the deviation of the time behaviour of P evaluated from measurements by means of eq.(1) from the function P(t) numerically calculated taking into account the spatial temperature profile.

From eq. (1) it follows that the frequency response of the bolometer, assuming a given $P(\omega)/A$ can be expressed by

$$T(\omega) = \frac{P(\omega)/A}{(c\varrho d)} \times \frac{\tau_c}{\sqrt{1+\omega^2 \tau_c^2}} \qquad (4)$$

In fact this is only the real part of the complex frequency response.

For $\omega\tau_c \ll 1$ a flat frequency response is obtained:

$$T(\omega) = \frac{P(\omega)/A}{(c\varrho d)} \times \tau_c \qquad (5)$$

which is independent of ω and is determined by

$$C/A = c\varrho d \qquad (6)$$

and

$$\tau_c = \frac{2a^2}{\pi^2 D} = \frac{A^2}{2\pi^2 D} \qquad (7)$$

τ_c includes the geometric dimensions of the surface (2a is the edge length of the quadratic bolometer foil) and the heat diffusion coefficient D (of the gold absorber).

For $w\tau_c \gg 1$ the limit is given by

$$T(\omega) = \frac{P(\omega)/A}{(c\varrho d)} \times \frac{1}{\omega} \qquad (8)$$

which is independent of τ_c and therefore of a and D, meaning that the bolometer integrates with respect to time the incident radiation power in this frequency range. From formulae (4) to (8) it can be seen that an increase of d makes the bolometer less sensitive (it should be noted that $c \times \varrho$ has the same order of magnitude for all materials used).

4.1 Calibration procedures

Two special cases of eqs. (1) and (2) are:

a) Dynamic case: P=0

This results in an exponential time decay of the foil temperature after screening off the incident radiation:

$$T(t) = T(t=0) \times \exp(-t/\tau_c). \qquad (9)$$

b) Stationary case: $P = P_{stat} = \text{const.}$

T reaches a saturation value which is proportional to the steady state power P_{stat}

$$T = P_{stat} \times z \qquad (10)$$

As can be seen, these two special cases can be utilized to determine the calibration constants z, C, τ_c.

To realize experimentally the dynamic case, one has to irradiate the bolometer surface uniformly and then turn off

the radiation power source on a time scale which is short compared with τ_c. From the cooling down curve of the bolometer one obtains τ_c (eq.(9)). For this calibration procedure we use a commercially available photo flashlamp or square wave excitation of the bolometer current. The time decay of the foil temperature after a tokamak discharge can also be used. The latter two methods have the advantage that they can be applied in-situ without removing the diagnostic apparatus from the machine.

To determine z(eqs.(10)and(12)) and, by means of eq.(3), hence C as well from the stationary case, one encounters the problem of depositing a power of known quantity on the bolometer surface. As first method, we use square wave excitation of the bolometer current to transfer an ohmic heating power of known quantity to the bolometer foil. Because the resistance layer is uniformly spread over nearly the whole surface, this approach towards simulating irradiation conditions is surely a good one. Additionally, we employ a second, independent calibration method: we blacken the bolometer surface with a thin layer of 'black gold' and illuminate it uniformly with light in the visible part of the spectrum. The intensity of this light beam can be measured with a calibrated power meter. At the moment we make the assumption that the light is totally absorbed by the blackened bolometer surface. In future we want to measure the reflection coefficient. A convenient method of doing this would be to compare the infrared emission of the blackened bolometer surface with that of a black-body reference source by means of an infrared camera (type AGA THV 780), assuming that the reflection coefficient in the visible is the same as in the 1 to 5 μm region.

This second stationary calibration method meets the conditions imposed on absolute calibration even better than the first. But, like dynamic calibration with a current pulse,

the ohmic heating method has the big advantage that it can be applied for all bolometers of an array simultaneously and in-situ, and because it can be automatically repeated many times the application of statistics will improve the accuracy. It affords a relative accuracy of better than 5 %, sufficient for Abel inversion or computerized tomography.

For absolute calibration we should additionally apply the light calibration method. The conversion factor between the results of the two methods should be the same for all bolometers and should not vary with time in view of the identical and highly reproducible design of the bolometers, which is also manifested in the scarcely differing calibration data. It is thus sufficient to determine the conversion factor just once in the laboratory using an arbitrary selection of all the bolometers used in measurements. At the moment, assuming the bolometers to be black, the result for the conversion factor is $z_{light}/z_{current} = 0.9$.

If a current I_B is passed through the bolometer, a resistance change ΔR caused by a temperature rise T of the foil results in an electric signal ΔU:

$$\Delta U = I_B \frac{dR}{dT} T \qquad \text{,where} \qquad (11)$$

$$\frac{dR}{dT} = \text{const.} \qquad \text{for a metal.}^{x}) \qquad (11a)$$

$\frac{dR}{dT}$ can also be measured in-situ by heating the whole bolometer head with a SS shielded thermocoax heating wire and simultaneously measuring the electrical resistance and the temperature, the latter with a SS shielded thermocoax thermocouple which is brought very close to the foil through a bore in the bolometer head (Sec.8.2)

$^{x})$ α in Table 1 means

(11b) $\alpha = \frac{dR}{dT} \times \frac{1}{R_o}$, where R_o is the linearly extrapolated resistance at a temperature of 0 °C.

From

$$z = \frac{dT}{dP_{stat}} = \frac{dR}{dP_{stat}} \Big/ \frac{dR}{dT} \qquad (12)$$

and formulae (10) and (11a) it is concluded that in the stationary case the resistance increase is proportional to P_{stat}:

$$\frac{dR}{dP_{stat}} = \text{const.} \qquad (12a)$$

The term "response" r is also often used in the literature:

$$r = \frac{dU}{dP_{stat}} = z\, I_B \frac{dR}{dT} \qquad (12b)$$

Summarizing eqs. (1) to (12), it is noted that the five calibration data C, τ_c, z, $\frac{dR}{dT}$, r are determined by three independent measurements, e.g. of τ_c, $\frac{dR}{dT}$, $\frac{dR}{dP_{stat}}$. They are listed in Table 1 and partly commented on in Sec. 3.1.

Our experiments in the laboratory and in Pulsator verified that $\frac{dR}{dT}$ and $\frac{dR}{dP}$ are indeed constants and the time decay of the bolometer temperature is exponential with sufficient accuracy, and that all the calibration data - which are listed in Table 1 - are reproducible within $\pm$ 10 %. Because the absolute and relative accuracy in measuring τ_c, z and C was not better than 5 to 10 %, the actual reproducibility of the bolometer data may even be better than the above quoted figure. The calibration data differ by the order of 100 % from those gained by calculation from the bulk material constants using eqs. (6) and (7).

In Sec. 5.3 we discuss in detail newly developed electronics for JET, the one output U_{SUM} of which is in first approximation directly proportional to the radiation power P absorbed by the bolometer, i.e. eq. (1) is solved by hardware:

$$P = \left[V \, I_B \, \frac{dR}{dP_{stat}} \, \frac{1}{\tau_c} \right]^{-1} \times U_{SUM} \qquad (13)$$

with

$$U_{SUM} = \left[\frac{d}{dt} U + \frac{1}{\tau_c} U \right]$$

where V is the amplification of the electronic circuit, and U/V is identical to the voltage ΔU of eq.(11). τ_c can be determined as described above but the whole factor $\left[V \, I \, \frac{dR}{dP_{stat}} \, \frac{1}{\tau_c} \right]$ can be obtained by a single calibration procedure, so that two steps are sufficient for the whole calibration.

5. Electronics

5.1 Origin of background signals

A signal estimate for JET (Sec.6) can be made more easily than an estimate of noise. In the latter one can only try to extrapolate experience gained in existing tokamaks. For this reason we discuss the detection limit in Pulsator /16/.

The detection limit of bolometer measurements in tokamaks is mainly governed by background signals caused by electrical pickup due to conductor loops, and, secondly, by common mode voltages in cases where the bolometer is not properly grounded.

Wherever possible, we can use highly twisted cables in the electrical circuit, but at the detector head itself and in the electrical vacuum lead-throughs, there is no way of avoiding open loops. An estimate shows that a magnetic field with a time derivative of 0.1 T/10 ms induces in a loop area of 1 cm^2 a voltage of 1 mV. This rough estimate reproduces, however, the background signal actually measured in Pulsator with reference to the amplifier input before we improved the signal-to-noise ratio (SNR) with a special electronic bridge circuit by an order of magnitude. In Pulsator the bolometer had the same electric potential as the vessel. Vessel voltages of, for example, 10 V can thus produce voltages at the amplifier input of 1 mV if the common mode rejection ratio (CMRR) is not better than 80 dB. During plasma build-up and disruption phases of Pulsator the disturbances caused by insufficient CMRR were even larger than those due to capacitive or inductive coupling or electronic noise.

In the case of JET, during a shot temperature drifts of the vessel and thermal loads on the bolometer due to penetrating neutron and γ-radiation (Sec.9.2) will give rise to additional disturbances which can reach the order of the measu-

ring signal.

Considering all these facts and bearing in mind that the bolometer signal, which still has to be detected, can be 10^{-4} to 10^{-5} of the voltage applied to the bolometer, it can be concluded that a compensation method employing a reference bolometer shielded against VUV radiation (see Sec.2) is absolutely necessary. In Pulsator we tested a prototype of this type of electronic bridge circuit with great success: the SNR was improved by a factor of 10, the background signal with reference to the amplifier input was 0.1 mV, which is the required 10^{-5} x U_B (U_B is the voltage across the bolometer). With the exception of the disruption phase (see above), the sum of background signal and noise was the same in Pulsator and in the laboratory, which means that, unlike with the electronics used before, the background signals are solely governed by the design of the electronics and no longer by disturbances specific to Pulsator.

5.2 Detection limit in Pulsator

In the Pulsator bridge electronics the output U_1 of the preamplifier was directly proportional to the resistance rise of the gold resistor above an equilibrium value and thus to the temperature increase of the bolometer foil. In the control room of Pulsator we differentiated this signal with respect to time and got by hardware the U_2 signal:

$$U_2 = c_1 U_1 + \frac{d}{dt} U_1 \qquad (14)$$

From eq. (1) it is seen that if c_1 is adjusted to make it equal to $1/\tau_c$, then U_2 is proportional to the radiation power absorbed by the bolometer. Both signals were measured by means of an oscilloscope after decoupling U_1 by linear optical decoupling, and U_2 by a modulation method applying vol-

tage-to-frequency conversion after the preamplifier in the torus hall and an 8-bit counter in the control room. For both signals the electronics had a flat frequency response up to 1 kHz, then a 6 dB/octave decline.

The detection limit of the U_1 signal was solely governed by the digit steps arising from the decoupling method applied, and, when converted to the preamplier input, was 100 µV. As we found above, this is 10^{-5} of the voltage across the bolometer resistance and corresponds to a detection limit of the bolometer temperature rise of 3.9×10^{-3} °C or an energy detection limit of 6.5 µJ or a stationary irradiation of the bolometer with 35 µW (Table 1).

The SNR of the U_2 signal was 12.5. This yields a detection limit of 270 µW, which corresponds to a bolometer temperature rise of 1.7×10^{-2} °C in steady state. The noise limiting the detectable signal can be quantitatively accounted for by the fact that the total noise of the preamplifier and the disturbances picked up in the transmission line are also differentiated.

5.3 JET electronics

The foregoing test results obtained in Pulsator pointed the way to new multichannel bridge electronics for JET (Fig.5). A prototype being constructed from it at the moment will be tested in ASDEX during 1980. A bolometer (R_B) and a reference bolometer (R_{RB}) shielded against VUV radiation are supplied by two independent current sources, each with a DC current of 2 mA stable to 10^{-5} because the resistance changes to be detected may be of this order of magnitude. Before every shot the bridge is automatically adjusted to zero output by re-adjusting the current with the reference bolometer.

During the plasma shot both currents are constant.

The signal S of the bridge, which is proportional to the resistance change of the gold resistor and thus to the temperature rise of the bolometer foil above the value before the shot, is preamplified by a differential amplifier, transmitted to the control area, decoupled, digitized and stored. This electronic channel carries all the information about the low-frequency part of the absorbed radiation power spectrum (eq.(5)). Because the frequency response of the bolometer declines in the high-frequency range as $1/\omega$ (eq.(8)), it is necessary, in order to measure this part of the spectrum as well with sufficient accuracy, to differentiate the signal S with respect to time and transmit $\frac{d}{dt}$ S separately via a second channel and decouple, digitize and store it. As seen in Sec.5.2, S has to be differentiated with respect to time before preamplification in order to avoid differentiation of the amplifier noise. Because a signal of the form U_2 in eq.(14) has the advantage of being directly proportional to the absorbed radiation power in a first-order approximation, it is proposed that the second electronic channel be designed in such a way that the signal S amplified by the factor $1/\tau_c$ is added to the signal $\frac{d}{dt}$S immediately after differentiation, resulting in a signal $\frac{d}{dt}$ S + $\frac{1}{\tau_c}$S (Fig.5). Both electronic channels have, in addition to a digital output, an analogue output, and the frequency response of both channels is flat up to 1 kHz, dropping thereafter by 6 dB/octave.

The solution of eq.(1) by hardware is an additional reason to that stated in Secs. 2.3 and 5.4 in order to balance the bridge to zero before each shot. There are also additional reasons for using not just one but two channels: a) equation (1) is - as quoted above - not quite correct, but laboratory experiments have shown that in the case of shot durations which are rather long compared with τ_c a correction term

containing S and due to heating of only the bolometer, but not the shielded reference bolometer has to be inserted in eq.(1); b) for determination of the calibration constant τ_c after the end of a shot the signal S is used; c) radiation energy bursts to the bolometer during disruptions may overdrive the amplifier of the $\frac{d}{dt}$ S channel, but the energy release of the plasma can then be determined from the jump in the S signal.

From Secs.5.1 and 5.2 it is obvious that the pinhole camera has to be electrically insulated from the vessel to form a Faraday cup. Nevertheless, both channels are decoupled before they are transferred to the control area. This prevents electrical loops in the multichannel circuit of a bolometer array and reduction of background signals due to capacitive coupling between the vessel and the pinhole camera. Should the voltages between the vessel and camera box be so high that flashover occurs, one must and can put the camera at vessel potential because of the decoupling. For the decoupling use is made of the method which was successfully applied for the U_1 signal in Pulsator employing voltage-to-frequency conversion immediately behind the preamplifier and counting, by means of a counter in the control area, the cycles during a time interval given by a 250 µs clock. The method has the advantage of good CMRR and avoids strong electrical pickup by way of the cables.

To avoid electric loops and also because the amplification factors to be set for the bolometers are different, the signals of different bolometers should not be multiplexed; what is needed is an electronic multichannel arrangement. The same electronic sub-units can be used for the bolometers of the arrays and for the single bolometers, thus allowing series production.

As indicated in Sec.4.1 (eq.(13)), the new electronics makes it possible to calibrate all bolometers of an array in-situ and simultaneously by raising the current stepwise in all bolometers by the factor F from a low value I_1 to the value I_2:

$$I_2 = F \times I_1 \qquad (15)$$

This results in heating of each bolometer foil. For example, the temperature rise for I_1 = 1 mA and I_2 = 2 mA is about 1.7 ^{o}C. Before the current is raised stepwise the bridge has to be balanced, and instead of the reference bolometer a calibration resistance R_{cal} is switched in which ought not to undergo any measureable heating due to the current step. If this is done, the factor $\frac{dR}{dP} \times \frac{1}{\tau_c}$ in eq.(13) can be determined. In the special case where the current step chosen is such that I_2 of eq.(15) is identical to I_B of eq. (13) and F is made just so large that the resulting heating of the bolometer foil has nearly the same magnitude as during a plasma shot, it is even possible to determine the whole factor $\left[V\ I_B \frac{dR}{dP_{stat}} \frac{1}{\tau_c}\right]$ in eq.(13):

$$\left[V\ I_B \frac{dR}{dP_{stat}} \frac{1}{\tau_c}\right] = U_{SUM} / \left[R_B I_B^2 (1-\tfrac{1}{F}2) + U_{SUM} I_B\right] \qquad (16)$$

where $U_{SUM} \times I_B$ is normally a small correction term. The bolometer resistance R_B and the current I_B through it have to be known. R_B can be obtained if the current through the calibration resistor R_{cal} is likewise fixed at a known value and the resulting bridge voltage is measured.

We propose electronics, using only two current values, the one of which (2 mA) is simultaneously used for measuring the plasma shots. The calibration accuracy aimed at is 5 %. It thus follows, for example, that the bridge has to be balanced with sufficient accuracy before triggering the current step

for calibration (eq.(15)), and secondly, the factor F has to be the same to a high degree of accuracy for both the bolometer and the calibration resistor, e.g. $\frac{\Delta F}{F}$ has to be 0.6×10^{-4} if I_2 = 2 mA and F = 2.

The electronics for JET has to be designed to allow complete remote control. All switching operations, particularly those concerning the part of the electronics in the torus hall, such as setting of all the currents and amplification factors, bridge balancing and interruption thereof, switching over from the reference bolometer to the calibration resistor, automatically applying the current step simultaneously for all bolometers and repeating it any number of times etc., have to be done by remote control.

All settings valid at a particular time can be read on the computer terminal of the operator. In the case of the current, not only the switch position but also the absolute current value should be measured and transmitted to the display. The remote control facilities for bolometric measurements in JET have to be newly developed and the technique to be employed therefore has to be decided during the preliminary design phase.

The cables inside the pinhole camera have to be fourstranded, highly twisted and insulated, and outside the camera they also have to be electrically shielded as far as the preamplifier. From the preamplifier on normal BNC cables can probably be used. More on this subject in Sec.8.1.

On the one hand, the preamplifiers have to be placed as close to the flange as possible. On the other hand, the biggest problem to consider in this context is that of radiation damage to the electronic components (Secs.9 and 9.1), which necessitates just the contrary, namely locating the preamplifiers in the basement of JET or in the torus hall behind a thick radiation protection wall.

In terms of the space required the electronics can be divided into two sections (Fig.5), the first located in the torus hall (or basement), the second in the control area. In the torus hall we need probably 11 NIM crates in a 19" rack, in the control room 5 NIM crates plus 1 CAMAC crate for data acquisition, likewise in a 19" rack.

5.4 Data acquisition

A data resolution of 8 bits at the beginning of JET operation will be sufficient because the dynamic range of the data can be kept small owing to the bridge balancing before the shot, transmission of both the S and the $\frac{d}{dt}$ S signals allows a smaller data resolution, and the SNR expected is small. But the system should be capable of extension to 12-bit words at any time without a great deal of extra outlay.

The electronic channels are connected to CAMAC memories where the data are collected during a shot. The samples are taken simultaneously for all channels. After a shot a computer reads the data and analyzes them. The sampling rate should amount to 1000 samples per shot, which means a sampling interval of 10 ms. In principle, a sampling rate of up to $(0.25\ \text{ms})^{-1}$ is possible on the basis of our electronic design. This meets the requirements of JET to have a variable sampling rate, controlled by an experimental parameter such as dI/dt (I: plasma current) which states how fast the plasma parameters vary with time. The electronics is thus flexible enough to study disruptions and MHD modes on a time scale of ms. For the sake of completeness, it should be noted that in our method the data resolution and sampling rate are correlated: e.g. 8 bits with $(0.25\ \text{ms})^{-1}$ and 12 bits with $(4\ \text{ms})^{-1}$.

Asssuming 4 arrays with 10 bolometers each plus 3 single bolometers, we need in the final stage 86 data channels with a total data amount per shot of 86 kwords or 172 kbytes.

6. Signal estimate

To get a convenient formula to estimate the bolometer signal strength, we treat the simpler case of a circular plasma cross-section. As the viewing field of the bolometer is limited by a slit-shaped diaphragm, every point of the bolometer sees a solid angle characterized by the angle 2α in the poloidal direction and 2β in the toroidal direction (Fig.6). We assume a radiation emission coefficient $\varepsilon(r)$, given in W/cm^3, which is only a function of the radius. The solid angle seen by the bolometer is

$$\Omega_B = 4\,\alpha\,\beta, \qquad \alpha \text{ and } \beta \text{ in units of arc,} \tag{17}$$

or else if α and β are sufficiently small,

$$\Omega_B = 4 \times \sin\alpha \times \sin\beta, \qquad \alpha \text{ and } \beta \text{ in degrees.} \tag{18}$$

The radiation power P_B received by the bolometer surface with area A_B is then

$$\frac{P_B}{A_B} = \left(\int_{\text{chord}} \varepsilon\, ds\right) \times \frac{\sin\alpha \times \sin\beta}{\pi} \tag{19}$$

where ε is integrated along the viewing chord through the plasma.

The assumptions underlying eq.(19) are that the bolometer surface is at right angles to the viewing chord, that, secondly, the plasma can be approximated by a cylinder and that, thirdly, 2α and 2β are sufficiently small.

If the entire plasma minor cross-section is now divided into parallel viewing chords (Fig.6) and their averaged intensity $\left\langle \int \varepsilon\, ds \right\rangle$ and a correspondingly averaged power absorbed per surface area $\left\langle \frac{P_B}{A_B} \right\rangle$ are introduced, we get

$$\left\langle \frac{P_B}{A_B} \right\rangle = \left\langle \int_{\text{chord}} \varepsilon\, ds \right\rangle \times \frac{\sin\alpha \times \sin\beta}{\pi} \tag{20}$$

Because of the assumed symmetry the plasma power P_p radiated in 2π from an arbitrary surface element A_p of the plasma is related to $\langle \int_{chord} \varepsilon \, ds \rangle$:

$$\frac{P_p}{A_p} = \frac{1}{\pi} \times \langle \int_{chord} \varepsilon \, ds \rangle . \qquad (21)$$

Combining eqs.(18), (20) and (21), the power absorbed per bolometer surface, averaged over all bolometers of an array, is

$$\langle \frac{P_B}{A_B} \rangle = \frac{P_p}{A_p} \times (\sin \alpha \times \sin \beta) . \qquad (22)$$

The value of $\frac{P_B}{A_B}$ obtained with this formula has to be substituted in the left-hand side of formula (1) to calculate the time evolution of the foil temperature. The two factors on the right-hand side of eq.(22) should now be treated in succession, first $\frac{P_p}{A_p}$, which is given by the plasma parameters, and secondly, the geometric factor $\sin \alpha \times \sin \beta$, which is determined by the bolometer aperture.

Table 2 presents typical JET parameters /1,2/. The heating power of 13 MW is composed of 3 MW of ohmic heating and 10 MW of additional heating, e.g. neutral injection. It is also a mean value of the target heating range of 3 to 25 MW. It should now be taken into account that only about 50 % of the quoted 6.5 W/cm^2 is lost by radiation, and so for JET we have to put 3.3 W/cm^2 for $\frac{P_p}{A_p}$ in eq.(22). If this value is compared with those of ASDEX: 2 $\frac{W}{cm^2}$ (1 MW heating power) and Pulsator: 1.85 $\frac{W}{cm^2}$ (110 kW heating power), it is seen that $\frac{P_p}{A_p}$ is of the same order of magnitude for all those machines which are very different in size and plasma parameters.

Table 2: JET parameters

R	296 cm
a	125 cm
b	210 cm
plasma volume	153.4 m^3
plasma surface	198.9 m^2
mean heating power	13 MW
power/volume	84.7 $\frac{mW}{cm^3}$
energy confinement time τ_E	1 s
shot duration	10 s
energy content = (heating power) x τ_E	13 MJ
power/surface (P_p/A_p)	6.5 $\frac{W}{cm^2}$

With $\sin\alpha \times \sin\beta = 1.3 \times 10^{-3}$ - a value which is mainly based on the assumption that there are 20 viewing chords per plasma cross-section with only a small overlap (Sec.8.1) - one obtains from eq.(22) $\left\langle \frac{P_B}{A_B} \right\rangle = 4.29 \frac{mW}{cm^2}$ which, in steady state, gives rise to a bolometer temperature increase of $T_{stat} = 0.17\ ^{o}C$.[x]) In Table 3 this value is compared with those measured in Pulsator /16/, and estimated for ASDEX.

Table 3 Bolometer signal estimate

	P_p/A_p	$\sin\alpha \cdot \sin\beta$	$\langle P_B/A_B \rangle$	T_{stat}
JET	3.3 W/cm^2	1.3×10^{-3}	4.29 $\frac{mW}{cm^2}$	0.2 ^{o}C[x])
ASDEX	2 W/cm^2	3.8×10^{-3}	7.6 $\frac{mW}{cm^2}$	0.7 ^{o}C
Pulsator	1.85 W/cm^2	1.2×10^{-3}	2.22 $\frac{mW}{cm^2}$	0.20 ^{o}C

We see that the bolometer temperature rise in the stationary phase of the gas discharge is the same in Pulsator as the value estimated for JET. The measuring time resolution in Pulsator was 10 ms. From this it follows that with the signal expected one should also reach 10 ms in JET.

The background signals in JET will, of course, be larger than in Pulsator but in Sec.5.3 we showed that the electronics to be used in JET will be a considerable improvement on that of Pulsator. Appropriate attention to the mechanical design extends the catalogue of steps taken to improve the SNR. Furthermore, one can look for a suitable metal resis-

[x]) It is taken into account that the JET bolometer with the 15 μm thick gold absorber will have a response which is only about 4/9 of the old one.

tor which has a higher temperature coefficient than gold (Table 1). It must, however, be stressed again that it is gold which endows the bolometer with such excellent properties as reproducibility and stability with time of the calibration data. If one opens the adjustable aperture of the pinhole camera and takes poorer spatial resolution into the bargain, one can also obtain better time resolution. The application of the bolometer pinhole camera in ASDEX will be a severe test for JET because in ASDEX the signal will be of nearly the same order of magnitude as in JET, but we are expecting larger background signals than in JET owing to the installation of the bolometer array within a region of high magnetic field strength and to the presence of an air-core transformer and shorter time constants for fluctuating magnetic fields.

During the preliminary design phase for the bolometric diagnostics the signal estimate presented in this section should be improved by numerical integration of several assumed radiation profiles over the non-circular plasma cross-section to yield signal strengths for distinct bolometer positions.

7. Multichannel arrangement of detectors

A serious diagnostic problem in JET is that the plasma is of a non-circular shape in the minor cross-section. A single array of detectors behind a common slit aperture and Abel inversion are thus no longer suitable means of determining the spatial distribution of radiation emission from multichannel measurement of plasma radiation emission along viewing chords. If no assumptions are made about the emission coefficient $\varepsilon(r, \Theta, t)$ in the poloidal plane, the method of computerized tomography /24,25,26/ would be capable of solving the problem of providing quantitative maps of the radiation emission coefficient in a single plasma plane from a large number of measurements of radiation intensities integrated along the viewing chords. For this purpose a large amount of detectors would have to be placed around the poloidal circumference of the plasma at different angular positions. But precisely this is impossible in the case of JET because of its limited port access. On the other hand, the measuring problem is considerably simplified if reasonable assumptions are made about the angular dependence of the emission coefficient, e.g. that it is relatively smooth /11,27/. In JET a tomography design study group is to make proposals for optimization of the number and arrangement of detectors with regard to the available geometry of JET. The results of this study are not yet available.

We thus proceed from the following assumptions: as already mentioned in Sec.2.2, to get contours of the emission coefficient in the poloidal plane, we have to scan the plasma in at least the horizontal and vertical directions. One pinhole camera should therefore be mounted at the horizontal port and one at the vertical port, each with an array of 20 bolometers mounted behind a common slit aperture. The bolometers of an array are arranged equidistantly on a semi-circle the centre of which is given by the aperture. Figures 8 and 10 show the proposed arrangement of bolometer detectors and

pinhole cameras in JET: for reasons set out in detail in Sec. 8.1 we recommend installing instead of the 2 cameras à 20 bolometers, 4 cameras à 10 bolometers. Only in the case of strong symmetry of radiation emission about the horizontal midplane would one of the two cameras at the horizontal port be redundant, but with two separate groups of detectors viewing the top and bottom halves of the discharge it is possible to check this symmetry.

The following particularities have to be considered when the tomography computer programs will be developed:owing to the V-shaped notch in the vessel the bolometers at the horizontal port are not able to view the plasma edge. This is even worse in the case of the vertically viewing bolometers. Then, only two quadrants of the plasma plane are totally covered by the two arrays; in the remaining two large edge regions are not covered. However, this should not be too bad because it can be assumed to first order approximation that the top and bottom halves of the plasma are symmetric and, secondly, the horizontally viewing arrays cover these edge regions. Another problem is that of overlapping viewing chords, which simply can no longer be mathematically treated as parallel chords. For a circular-shaped plasma the problem is treated in Ref. /28/. An appropriate method for non-circular cross-sections has to be developed. Another effect is sketched in Fig.7. One can realize the angle 2α, which determines the radiation power P on the bolometer surface (eq.(19)) and hence the bolometer signal, either with aperture No.1 or with No.2. But, because of the not infinitely small extent of the bolometers the angles α and γ are different, the difference increasing with decreasing distance of the bolometer from the aperture. 2γ limits the field of view and the case $\gamma \neq \alpha$ may possibly cause a small correction to the radiation power evaluated from eq.(19). The reason for this correction is that the bolometer signal is in fact proportional to the radiation power P averaged over the bolometer surface. If different surface elements view different plasma regions, this can cause nonuniform irradiation of the surface.

8. Mechanical design

8.1 The JET bolometer pinhole cameras

The bolometer pinhole cameras are symmetrically mounted to the top and bottom of the horizontal port of JET on both sides of the flange centre, in such a way that each of them covers half of the poloidal plasma cross-section (Fig.8). When viewed from above, the pinhole cameras have to be in the flange centre (Fig.9). One vertical port should be exclusively reserved for two pinhole cameras each of them covering half of the plasma cross-section (Fig.10) [x]) and whose viewing chords are directed vertically. In each pinhole camera there is an array of 10 bolometers arranged equidistantly on a semi-circle around a rectangular slit aperture, making a total of 40 bolometers scanning the plasma minor cross-section.

This solution for the detector arrangement meets, in addition to the requirements imposed by the measuring objective (Sec.7), some other important boundary conditions required of the bolometer pinhole cameras in JET: The camera box together with the aperture system has reasonable dimensions allowing both the space required to be kept to a minimum and the onset of mechanical vibrations during shots to be largely suppressed. The impairment of other diagnostics at the horizontal port is considerably reduced by locating the pinhole camera at the edge of and outside the flange behind a valve. The latter still affords particularly good access to the camera for remote handling operation and ensures, at least in the case of the bolometers at the horizontal port, that they are located at a distance of more than 6 m from the torus centre and hence in a region of small vertical magnetic field /29/.

---

[x]) If remote handling requirements do not prevent this, we should like to use the bottom port (instead of the top) because in this case the cable length to the preamplier is shorter.

This guarantees that the pickup signals due to the loop areas formed by bolometer contacts and vacuum feedthroughs are minimum. The desire to place the bolometers in regions of small vertical magnetic field cannot be fulfilled with certainty in the case of the pinhole cameras at the vertical port because at present JET cannot provide us with two-dimensional maps of the vertical magnetic field and its time behaviour. At present two different types of pinhole cameras are envisaged. During the final mechanical design an attempt should be made to apply four identical camera boxes to JET, only the aperture being different, to facilitate replacement of cameras in the event of repair and maintenance. One bolometer array would always be in reserve to continue measurements without delay.

Compared with the ASDEX pinhole camera /16/, JET involves new aspects or old ones had to be re-weighted, i.e. the camera had to be redesigned. In Fig.11 the camera destined for the horizontal port is shown in detail. The bolometers are mounted 44 cm behind a rectangular slit aperture of 30 mm (poloidal) x 33.8 mm (toroidal). $\sin\alpha \times \sin\beta$, which determines the bolometer signal (eq.(19)), is for the bolometer viewing the centre 1.3×10^{-3} (see Table 3) and the spatial resolution of this bolometer on the plasma axis is 28 cm. We thus have a small overlap of viewing chords (Fig.8), but we need as large a solid angle as possible for intensity reasons (Sec.6). β is limited by the V-shaped notch of the vessel - this cause of the intensity limitation also being the reason why the pinhole camera should not be moved from the flange centre (Fig.9). α is limited by the need to have 10 chords per half of the plasma cross-section which just overlap.

The cameras at the vertical port have geometrical dimensions different from those at the horizontal port. The bolometer

array is mounted 60 cm behind a slit aperture of 30 mm x 30 mm (20.6 mm)[x]), yielding a value for sinα x sin ß of 6.2 x 10^{-4} (4.3×10^{-4})[x]) and a spatial resolution on the plasma axis of 18.5 cm (Fig.10).

Sinα x sin ß will thus be smaller than in the case of the cameras at the horizontal port, and may possibly even be intolerably small if we retain the requirement that there be 20 nearly non-overlapping viewing chords through the vertical port (limitation for α). It thus seems inevitable that the aperture width will have to be increased to gain a larger signal at the cost of spatial resolution. But this should be decided after the first experimental results from ASDEX are available. In any case the apertures of all the pinhole cameras are measurably adjustable in the poloidal direction, i.e. in the case of very small signals the aperture can then be opened at the expense of the spatial resolution. Like all mechanical manipulations of the camera this has to be done by remote control. The aperture edges are designed to afford easy replacement.

To build the camera including the aperture as a Faraday cup reducing electric stray fields in the interior of the camera as far as possible, electrical insulation will have to be provided when attaching the camera to the JET vessel. Our experience with Pulsator (Sec.5.1) makes this absolutely necessary. It still has to be clarified how this insulation can be achieved, but a metal-coated ceramic insulator may afford a solution.

---

[x]) The values are generally presented in the same order as in the previous section. The figure in parentheses refers in each case to the second of the two cameras at the vertical port because, in view of the fact that the vertical port viewed from above is wedge-shaped, thus limiting the field of vision (angle ß), we have to apply two different aperture widths in the toroidal direction for the two cameras.

The camera box and the metal rail on which the bolometers are mounted have to be cooled with a water cooling circuit down to 50 °C because the bolometers cannot be baked to 500 °C like the vessel (see Sec.3.1). Probably the use of tritium (Sec.9.3) will impose special requirements on the cooling circuit and this point will have to be specified more clearly by JET. The same circuit should also be used for baking the camera to 200 °C after ventilation and before the separation valve is opened. This will do to evaporate the water absorbed from the air by the capton foil of the bolometer.

The pinhole camera is connected to the vessel by way of a bakeable, metallic separation valve /30/. This valve serves only for maintenance, repair and cases of emergency; its number of operations will be strictly limited. An automatic closing procedure has to be provided for the separation valve in the event of leaks in the diagnostic attachment. Because parts of the cameras penetrate through the open separation valve, compulsory interlocks have to be provided in order to prevent mechanical damage. The whole of the front part of the camera including the aperture is shifted back and forth by a compressed-air-driven pneumatic cylinder, a (probably double-walled) bellow being incorporated for this purpose (Fig.11).

In addition to the valve described, the camera is equipped with a remote-controlled flap valve. It does not have to shut vacuum-tight, but it does have to shield the camera inside against discharge cleaning and titanium evaporation and can be used to discriminate background signals from measuring signals. It can be closed between shots. The aperture of the camera also acts as a pumping port. Because of the small aperture size and to afford the possibility of pumping the camera after ventilation, auxiliary contamination-free turbomolecular pumps are connected to the camera by way of sepa-

rate pumping ports. The pumping system has to be tritium compatible and only metal gaskets will be used /30/.

The bolometers are mounted on the metal rail in such a way that they have very good thermal contact with it. The reference bolometers are placed immediately next to the bolometers and are shielded against VUV radiation by an approximately 1 mm thick wafer of gold-plated copper. The loops formed by the contact pins, in the bolometer and reference bolometer, are parallel to the vertical magnetic field to minimize pickup, a principle which has been outstandingly successful in Pulsator.

All bolometers and reference bolometers can be detached singly. To allow this by remote handling during D-T operation of JET, the detector head (Fig.2) has to be modified in such a way that a manipulator can insert and withdraw the plug connection. In the event of several bolometers being damaged the whole pinhole camera is detached from the vessel by remote handling, after the valve has been closed. With the flap valve closed to reduce outgasing of tritium, the camera will then be transported to a hot cell, where it will be opened. The bolometer array mounted on the flange cover is then accessible from the front for individual dismantling of detectors by remote handling. The mounting rail in the pinhole camera will be adjusted only once during commissioning of the pinhole camera in JET. The design will ensure that the same setting can be obtained with sufficient accuracy at any time when replacing the array later.

It should be noted that several thermocouples should be provided to afford remote monitoring of the temperature of the camera box and of the bolometers, and that cable strands, compressed-air lines and cooling water pipes have to be directed to the pinhole cameras. The camera should be made of electropolished stainless steel with a relative magnetic

permeability of less than 1.05. The cable insulations have to be selected with great care. In Sec.5.3 it has already been stated that we need 4-stranded, highly twisted, insulated cables inside the camera. Cable insulations can outgas considerably and mostly they are not resistant to heat, tritium and nuclear radiation. This makes further tests on cables necessary. Possibilities are afforded by ceramic-insulated cables and mineral-insulated cables with stainless steel sheath. Problems will arise in twisting these cables.

The port the bolometer cameras should be attached to should meet the following requirements: no cold gas inlet or limiter should be in the neighbourhood because both can falsify the bolometer signal, owing to an atypical neutral particle background. The aperture of the pinhole camera ought not to be bombarded by the neutral injection beam, just as all applied heating methods should not act directly on the camera and generate a bolometer background signal. Spectroscopic measurements at the same port would be desirable to have an improved possibility of comparison.

8.2 The single bolometers

In Sec.2.2 we have already stated some of the reasons for installing in JET several single bolometers distributed around the toroidal circumference, each of them seeing the whole plasma minor cross-section: as a test of toroidal symmetry of the radiation emission, normalization of the scan results obtained by means of the pinhole cameras, improved measuring time resolution, discrimination of radiation from the low-energy part of the spectrum, and extension of the spectrum range covered to the infrared.

The mechanical design of the single bolometers for JET is not included in this design study but it will have to be checked

during the 'preliminary design phase' whether the principles on which the mechanical design of the single bolometers for ASDEX is based can be retained - though it is already evident that the details of the design will have to be drastically modified. The design for ASDEX is therefore now briefly described (Fig.12).

Located adjacent to the bolometer is a reference bolometer permanently shielded against VUV radiation. In front of the two is a rotary aperture disc equipped with different replaceable apertures and filters: In the 'closed' setting the aperture disc performs the same function as the flap valve of the pinhole camera (Sec.8.1). In the 'open' setting each surface element of the bolometer views the total plasma minor cross-section. In the toroidal direction a well-defined plasma region is stopped down to enable spatial resolution in this direction, to simplify data evaluation (e.g. validity of the assumption that the plasma is cylindrical in shape) and to guarantee uniform irradiation of the bolometer surface. The design of the aperture also ensures that charged particles tied to magnetic field lines cannot hit the bolometer if the whole device is within the vessel. In the 'filter' position a very thin filter foil (e.g. 0.1 μ thick Be or C) is inserted in the radiation path to absorb the low-energy part of the radiation, thus allowing measurements with a rough energy resolution by means of filters of different thickness. The heating wire and the thermocouple are incorporated primarily to allow in-situ determination of dR/dT (Sec.4.1, eq. (11)); since we have developed new electronics (Sec.5.3) this reason ceases to apply.

With regard to electrically insulated installation of the apparatus on the vessel and water cooling of the device, electrical cables and vacuum feedthroughs, separation valves

and compulsory interlocks, and, last but not least, remote handling in the event of damage, the statements made in Sec.8.1 are valid for the single bolometers as well. The biggest problem that has to be solved first is that the entire single bolometer unit has to be installed deep in the port of the JET vessel so that the uniformly irradiated bolometer views the whole plasma minor cross-section. This geometric arrangement greatly aggravates the problem of solving the technical difficulties just outlined that are already present.

The signal of the single bolometers should be an order of magnitude larger than the signals of the pinhole camera bolometers owing to the increased aperture width in the poloidal direction. If a better SNR results from this, an improved measuring time resolution can be achieved. But it has to be noted that there is likewise an increase of the background signals if the bolometers are located inside the port in regions of highly fluctuating magnetic fields. To measure the radiation power emitted between about 2000 Å and the infrared, one should compare two single bolometer signals measured simultaneously at the same toroidal angle, one obtained with an unblackened and the second with a blackened single bolometer (Sec.3.1).

One problem concerning data evaluation should be mentioned: If the distance between the bolometer and plasma is not sufficiently large, then, even with a clearly defined aperture geometry, one cannot uniquely determine the total plasma radiation losses from the measured bolometer signal, but the spatial distribution of the radiation emission enters into the calculation.

9. D-T operation

In its final experimental phase JET will be operated with a D-T mixture. In this mode of operation the maximum neutron and γ-fluxes will be generated. Over a period of 2 years it is planned to perform 1o,ooo shots with the D-T mixture, each shot producing $1o^{2o}$ neutrons/shot /1,31/ . The latter has to be considered as the maximum credible neutron production rate. In the D-D operation mode the neutron production will be 3 orders of magnitude lower. For a plasma surface of about 2oo m^2 the unscattered neutron flux at the surface will be $5 \times 1o^{12} \frac{n}{cm^2 \times s}$ or $5 \times 1o^3$ rad/s, if we make use of 1 rad = $1o^9$ n/cm^2, which is valid for CH material /32,33/. Taking into account the backscattered neutrons, the total neutron flux may be a factor of about 5 to 10 higher if we adopt the ratio of unscattered to backscattered neutron flux as calculated for ZEPHYR /34/. Thus, the above quoted 1o,ooo shots will produce a total amount of about $2.5 \times 1o^{18} \frac{n}{cm^2}$ or, correspondingly, $2.5 \times 1o^9$ rad. The bolometers in direct visual contact with the plasma are fully exposed to this radiation flux. Owing to collision processes the primary neutron energy spectrum will be smoothed and will be similar in shape to that of a fission reactor - although it has to be borne in mind that most of the published neutron spectrum calculations /34,35/ were made to obtain the irradiation of magnetic field coils, outside the vacuum vessel.

The neutron fluxes already cause after a few D-T shots activation of the machine, which prevents personnel from having access to the torus hall and necessitates remote control of all diagnostics attached to the machine (Sec.8). In the event of damage, the replacement and repair of these diagnostics have to be done by remote handling. Fast

neutrons can cause severe radiation damage in many materials, and electronic components, in particular, have to be carefully shielded against neutron radiation.

The γ-radiation is caused, on the one hand, by bremsstrahlung und line radiation during a plasma shot and, on the other, by (n, γ) processes or inelastic scattering from the vessel wall or support structure. γ-radiation can cause radiation damage just like neutrons, but the activation of materials due to γ-radiation is negligible.

Two questions arise: Is the bolometer insensitive enough to radiation damage and what radiation shielding procedures have to be adopted for the electronics in the neighbourhood of the vessel?

9.1 Radiation damage

Considering that the effects of neutrons and γ-radiation on matter are different, that slow and fast neutrons show different behaviour, and that metal and polymeric materials react differently to radiation, it can be seen how complex the problem of radiation damage is.

First we treat the effect of neutrons on metals. Transmutation processes (n,γ) due to slow neutrons as well as ionization processes due to neutrons and γ-radiation can be neglected. When, however, fast neutrons above 1 MeV collide with lattice atoms, they can eject these atoms from their lattice positions, and the atoms, in turn, can collide with new atoms, producing Frenkel pairs /36/. A convenient measure of the abundance of these processes is d.p.a. (displacements per atom), a quantitiy which is proportional to the neutron dose given in n/cm^2. If one summarizes the values in the literature (e.g. /33,37 to 39/), neutron doses of $1o^{18}$ to $1o^{19}\frac{n}{cm^2}$ ($1o^{18}\frac{n}{cm^2}$ corresponds to

about 5,ooo D-T shots in JET) are necessary to produce resistance changes in metals of the order of 0.1 to 1 %.

Semiconductors are much more sensitive to radiation damage than metals(/33,38,39/) because ionization effects become very important and lattice distortions or impurities induced by nuclear reactions have an enormous influence on their electrical properties. A neutron dose released during one D-T shot in JET ($2.5 \times 1o^{14} \frac{n}{cm^2}$) can produce an irreversible resistance change of the order of about five per cent in materials such as Ge. The reversible resistance change during plasma shots can be even orders of magnitude higher.

Radiation damage in capton, which belongs to the polyimide group,is studied in detail because it is used as a cable insulation in fission reactors and particle accelerators. In Ref. /4o/ radiation damage in polymeric materials is reviewed and capton is treated in detail. The dose unit 1 rad corresponds to 1oo erg of absorbed energy in 1 g of matter /36/. Rad is a suitable unit for describing radiation damage in polymeric materials because it is a rule of thumb that a certain amount of absorbed energy per unit mass causes in polymerics a certain degree of damage, irrespective of whether neutron or γ-radiation is involved and of which part of the energy spectrum the radiation is located in /33/. The main types of radiation damage are ionization of the polymeric material, excitation or even dissociation of molecules, and formation of free radicals which will react with each other or with their surroundings, undergoing cross-linking or degradation. To summarize results published in the literature (Ref. /33,4o to 43/), capton (chemical symbol $(C_{22}H_{1o}N_2O_4)_n$) can be used without trouble up to radiation doses of $5 \times 1o^9$ rad, which corresponds to 2o,ooo D-T shots in JET, during which capton would not lose its mechanical strength and electrical insulation properties.

Summarizing this section, we can state that the metal bolometer described in Sec. 3.1 should withstand about 2o,ooo D-T plasma shots in JET without being damaged or losing its properties.

What has been said concerning the bolometer applies equally well to the electronics, which is exposed to neutron and γ-radiation. The electronics has to be radiation shielded by thick walls consisting, if possible, of boronated concrete and lead. The exact composition and thickness of the wall can only be specified when the location of the preamplifiers has been fixed and for this well defined position the neutron and γ-dose rates during plasma shots have been calculated. In any case it must be possible to replace the electronics for repair or when its performance degrades. To facilitate access in such cases, we prefer locating the bolometer preamplifiers in the torus hall in a radiation-shielded rack. To save space, it is certainly advisable to include the bolometer electronics together with that of other diagnostics in several racks and provide them with common shielding. Problems entailed in locating preamplifiers and shielding them from radiation which are common to several diagnostics, should be investigated by JET to provide recommendations of specific techniques.

Despite the fact that the test results are excellent for our purpose, the metal resistor bolometer should be tested in the neutron and γ-flux of a fission reactor. At the Garching reactor (FRM) there is a group which has a lot of experience in studying high-dose irradiation effects in metals (at low temperatures) /44/. Using nearly the same experimental equipment as they do, we could irradiate the bolometer for some hours to simulate JET irradiation conditions and test the behaviour of the bolometer by in-situ measurement of electrical resistance and temperature.

9.2 Energy depositon by neutron and γ-radiation

The high-energy neutron and γ-radiation generated during a plasma shot penetrates the walls of the vacuum vessel and pinhole camera. This neutron and γ-radiation emitted from the whole of the plasma volume irradiates each bolometer and deposits energy in the bolometer foil by volume absorption: 1 mW of power absorption per 1 mg of material is equal to 10^5 rad/s (Sec.9). In the case of ZEPHYR this phenomenon was carefully studied (Sec. 2.4 of Ref. /34/). The authors show that in stainless steel 80 % of the energy deposition rate is due to γ-radiation and only 20 % is caused by neutrons. In the case of hydrogen-rich material such as epoxy it is just the opposite - 85 % of the deposited energy is from neutrons, and 15 % from γ-radiation. The photon contribution in units of W/g is quite independent of the material, whereas the neutron contribution strongly dominates in hydrogen-rich plastic material.

If we take the data from Ref. /34/ and assume that the energy deposition rates in JET are a factor of 50 lower than in ZEPHYR (the ratio of the unscattered neutrons in the two tokamaks amounts to 50), we can very roughly estimate that the temperature rise of the bolometer foil caused by nuclear heating during a shot may be of the same order of magnitude as the measuring signal originating from absorption of VUV radiation. Thus, to eliminate background signals an efficient compensation method such as that described in Secs. 2.3 and 5.3 must of necessity be applied. In connection with the fission reactor test (Sec. 9.1) the problems stated should be experimentally investigated in more detail.

9.3 Tritium

The technical problems caused by the use of tritium in JET are described in Ref /1/. One of the properties of tritium is that it can replace normal hydrogen in chemical

compounds by isotopic exchange reactions. It is generally known that this can give rise to degradation of polymeric materials if a high tritium pressure ensures a sufficiently high concentration of tritium in the material. This effect has to be taken into account with respect to the capton of the bolometer and all organic insulations used in building the pinhole camera. For capton (polyimides) no experimental data have been published. One conceivable effect of applying the bolometer in the tokamak is that high-energy tritium atoms from the plasma will be injected into the foil and, in view of their relatively high solubility in capton, will build up a high tritium concentration. It must, of course, be considered that the 15 µm thick gold surface layer constitutes a permeation barrier.

With a simple tritium test in which molecular tritium is allowed to act on the bolometer, this effect could not, for instance, be simulated, nor is it at all certain whether a sufficiently high tritium concentration can be achieved by this test method.

In the event of repair of the bolometer pinhole camera or replacement of bolometers the greatest risk is that tritium can outgas from the opened device and, in the form of tritiated water, pollute the air. In such work all safety precautions envisaged in JET for this case have to be observed.

The auxiliary pumping circuit has to be of tritium-compatible design (see Ref. /3o/). It has to be ensured that tritium cannot escape from the bolometer device, e.g. from the cooling circuit into the heat exchanger system (a closed loop system is necessary), and all walls of the vacuum system have to be thick enough to prevent permeation through them.

Acknowledgement

The author wishes to acknowledge the continuous support of the scientific and technical staff of ASDEX in the preparation of this study. He is also indebted to D.E.Groening of the electronics workshop and to R.Komen for many clarifying discussions of the electronic and mechanical design of the multichannel bolometer diagnostics. He thanks C.K. Shie who tested experimentally the calibration procedures and made many helpful suggestions. He is also grateful to H.Weichselgartner for contributing know-how on radiation damage due to tritium. The mechanical design for JET was carried out under the supervision of H.Goss.

References

/1/ The JET Project Design Proposal, Rep.EUR-JET-R5, Culham (1975)

/2/ The JET Project Scientific and Techn.Developments, Rep. 5791 e, Culham (1977)

/3/ T.F.R.Group, 6th Conf.on Plasma Phys.and Contr.Nucl. Fusion, Berchtesgaden (1976)Paper IAEA-CN-35/A3

/4/ K.Bol, et al., 7th Conf.on Plasma Phys.and Contr.Nucl. Fusion, Innsbruck (1978) Paper IAEA-CN-37-A-1

/5/ H.Eubank, et al., 7th Conf.on Plasma Phys.and Contr. Nucl.Fusion, Innsbruck(1978), Paper IAEA-CN-37-C-3

/6/ J.Hugill, et al.,8th Conf.on Contr.Fusion and Plasma Phys., Prague (1977), I 39

/7/ L.A.Berry, et al.,6th Conf.on Plasma Phys.and Contr. Nucl.Fusion, Berchtesgaden (1976) Vol.1, p.49

/8/ WVII-A Team,7th Conf.on Plasma Phys.and Contr.Nucl. Fusion, Innsbruck(1978), Paper IAEA-CN-37/H2

/9/ J.W.M.Paul, 6th Conf.on Plasma Phys.and Contr.Nucl. Fusion, Berchtesgaden(1976),Paper IAEA-CN-35/A17

/10/ C.E.Bush, J.F.Lyon, ORNL Report ORNL/TM-6148, Oak Ridge (1977)

/11/ N.R.Sauthoff, Proceed.of the Society of Photo-Optical Instrumentation Engineers 106, 40 (1977)

/12/ L.E.Sharp, L.S.Holmes, P.E.Stott, D.A.Aldcroft, Rev. Sci. Instrum., 45, 378 (1974)

/13/ H.Jäckel, H.Krause (private communication)

/14/ H.Hsuan, K.Bol, R.A.Ellis, Nucl. Fus. 15, 657 (1975)

/15/ T.F.R.Group, Nucl.Fus. 18, 647 (1978)

/16/ E.R.Müller (to be published)

/17/ P.Ginot, Internal TFR Report NT/178, Fontenay aux Roses (1977);
A.L.Pecquet (private communication)

/18/ G.B.Sabine, Phys.Rev. 55, 1064 (1939)

/19/ WM J.Veigele, Atomic Data 5, 51 (1973)

/20/ W.C.Walker, O.P.Rustgi, G.L.Weissler, J.Opt.Soc.Am. 49, 471 (1959)

/21/ L.Harris, et al., J.Opt.Soc.Am., 38, 582 (1948)

/22/ J.F.Schivell (private communication)

/23/ J.Hugill, A.L.Pecquet (private communication)

/24/ W.Swindell, H.H.Barrett, Phys.Today 30, 32 (1977)

/25/ Z.H.Cho, Ed., IEEE Trans.Nucl. Sci., NS-21 (1974)

/26/ A.M.Cormack, J.Appl.Phys. 34, 2722 (1963)

/27/ N.R.Sauthoff, S.v.Goeler, IEEE Trans.Pl.Sci., PS-7, 141 (1979)

/28/ P.Smeulders, IPP Report IPP 2/240, Garching (1978)

/29/ G.Magyar (private communication)

/30/ G.Venus, K.J.Dietz, Internal JET Report JTN/C(79) 138, Culham (1979)

/31/ P.E.Stott, Internal JET Diagnostic Memo 5, Culham (1979)
A.Gibson, Internal JET Diagnostic Memo 6, Culham (1979)

/32/ S.Nishijima, T.Okada, Cryogenics 18, 215 (1978)

/33/ S.Battisti, R.Bossart, H.Schönbacher, M.Van de Voorde, CERN Report 75-18, Geneva (1975)

/34/ H.Brockmann, H.Krause, U.Ohlig,
Internal ZEPHYR Report No. 5, Garching (1979)

/35/ G.M.McCracken, S.Blow, CLM Report CLM-R 120, Culham(1972)

/36/ L.Bochirol, et al., CERN Report 77-03, ed. by M.Van de Voorde, Geneva (1976)

/37/ B.McGrath, H.Schönbacher, M.Van de Voorde, Nucl. Instrum. and Methods 136, 575 (1976)

/38/ A.de Combarien, M.Van de Voorde, CERN Report 77-03, ed. by M.Van de Voorde, Geneva (1976)

/39/ Effects of Radiation on Mat.and Compon., ed by J.F. Kirchner,R.E.Bowman,Reinhold Publ.Corpor. New York

/40/ M.H.Van de Voorde, CERN Report 70-5, Geneva (1970)

/41/ D.C.Phillip, AERE Report R8923, Harwell (1978)

/42/ M.H.Van de Voorde, C.Restat,CERN Report 72-7, Geneva (1972)

/43/ H.Schönbacher, Bull. SEV/VSE 69, 2 (1978)

/44/ M.Nakagawa, K.Böning, P.Rosner, G.Vogel, Phys.Rev. B16, 5285 (1977)

Figure Captions

Fig. 1 Bolometer foil (schematic)

Fig. 2 The bolometer

Fig. 3 Total attenuation cross-section of gold in the photon energy region 0.1 to 10 keV (from Ref. /19/)

Fig. 4 Reflectivity of gold in the spectral range 400 Å to 4800 Å (from Ref./18/)

Fig. 5 Bolometer electronics for JET

Fig. 6 Spatial resolution of measurement (schematic)

Fig. 7 Effect of not infinitely small bolometer surface

Fig. 8 The two bolometer pinhole cameras at the horizontal port of JET (poloidal cross-section)

Fig. 9 Bolometer pinhole camera at the horizontal port of JET (toroidal cross-section)

Fig. 10 The two bolometer pinhole cameras at the vertical port of JET

Fig. 11 Preliminary design of the bolometer pinhole camera at the horizontal port of JET

Fig. 12 Single bolometer unit for ASDEX

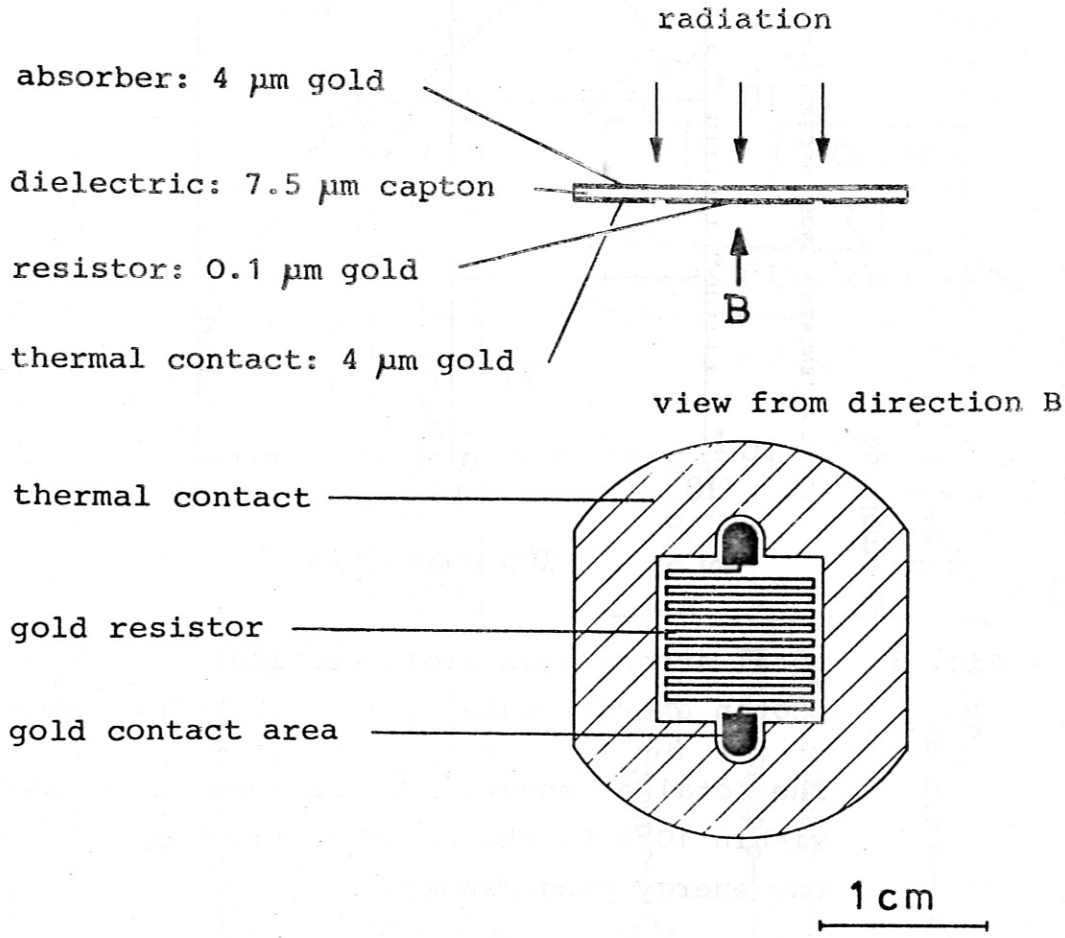

Fig. 1 Bolometer foil (schematic)

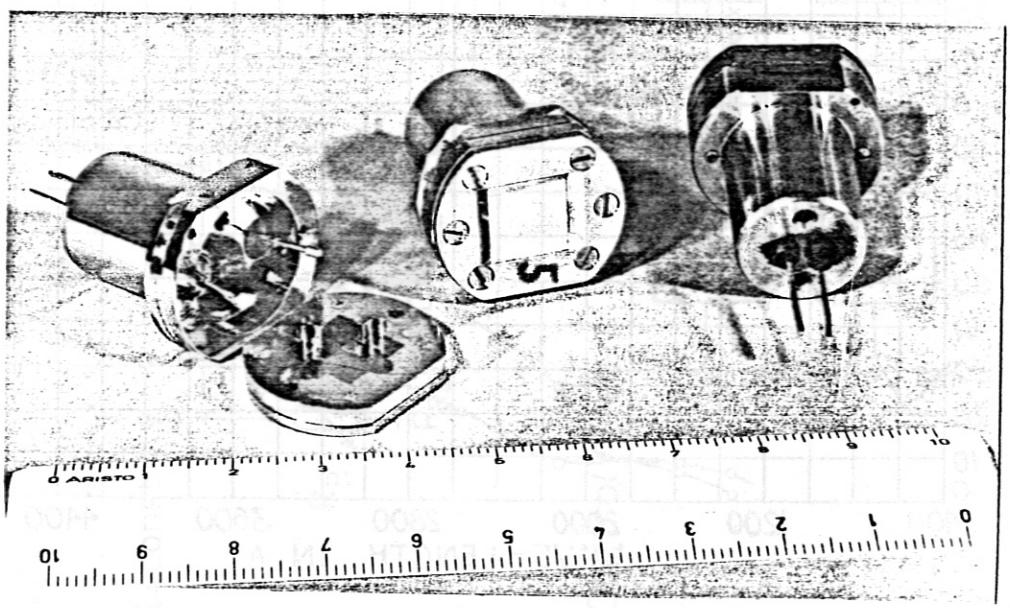

Fig. 2 The bolometer

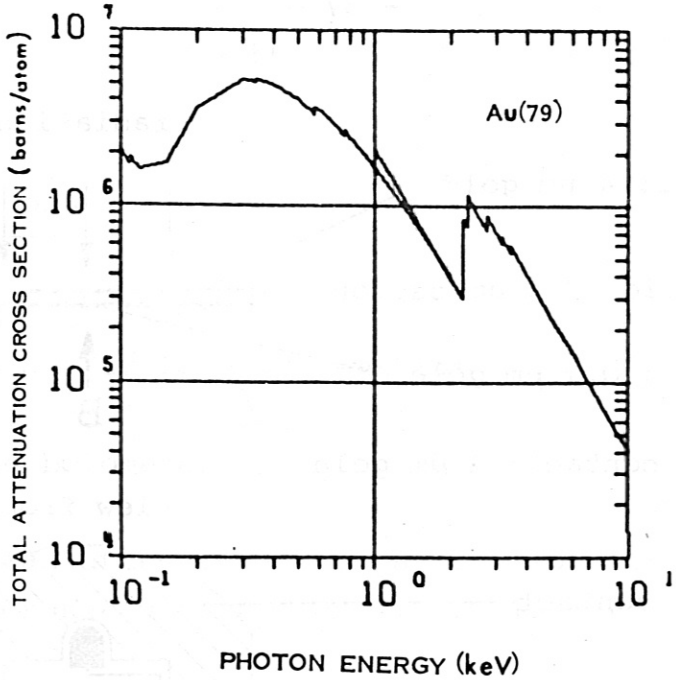

Fig. 3 Total attenuation cross-section of gold in the photon energy region 0.1 to 10 keV (from Ref./19/)

The total attenuation cross-section is identical within 10 % to the photoelectric cross-section in the energy range shown.

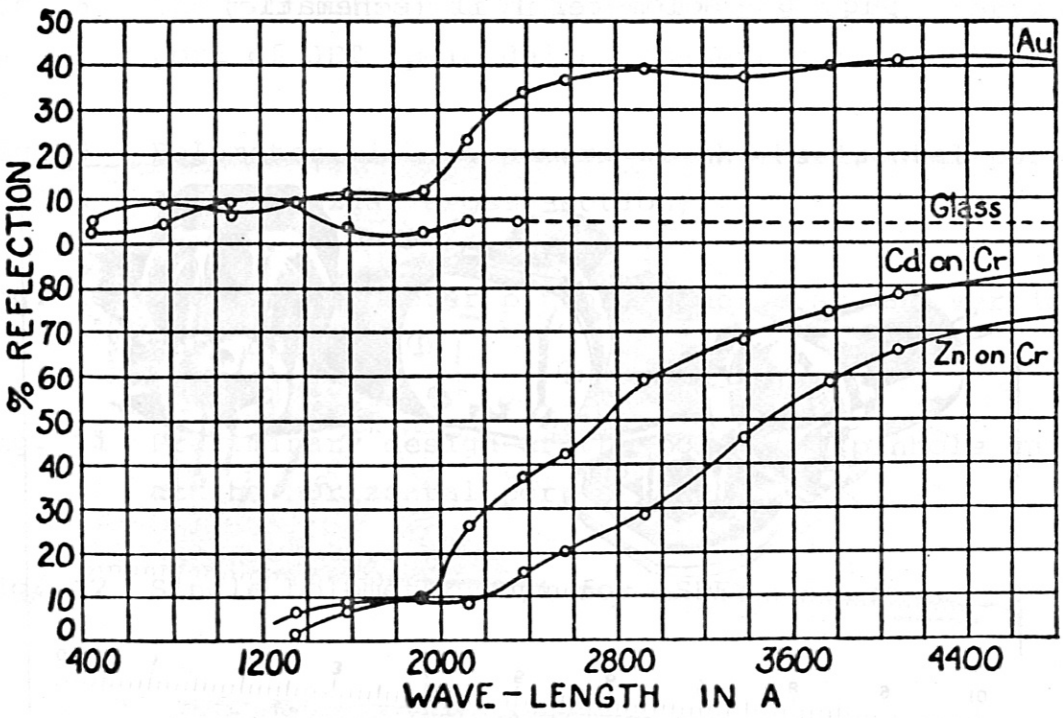

Fig. 4 Reflectivity of gold in the spectral range 400 Å to 4800 Å (from Ref./18/)

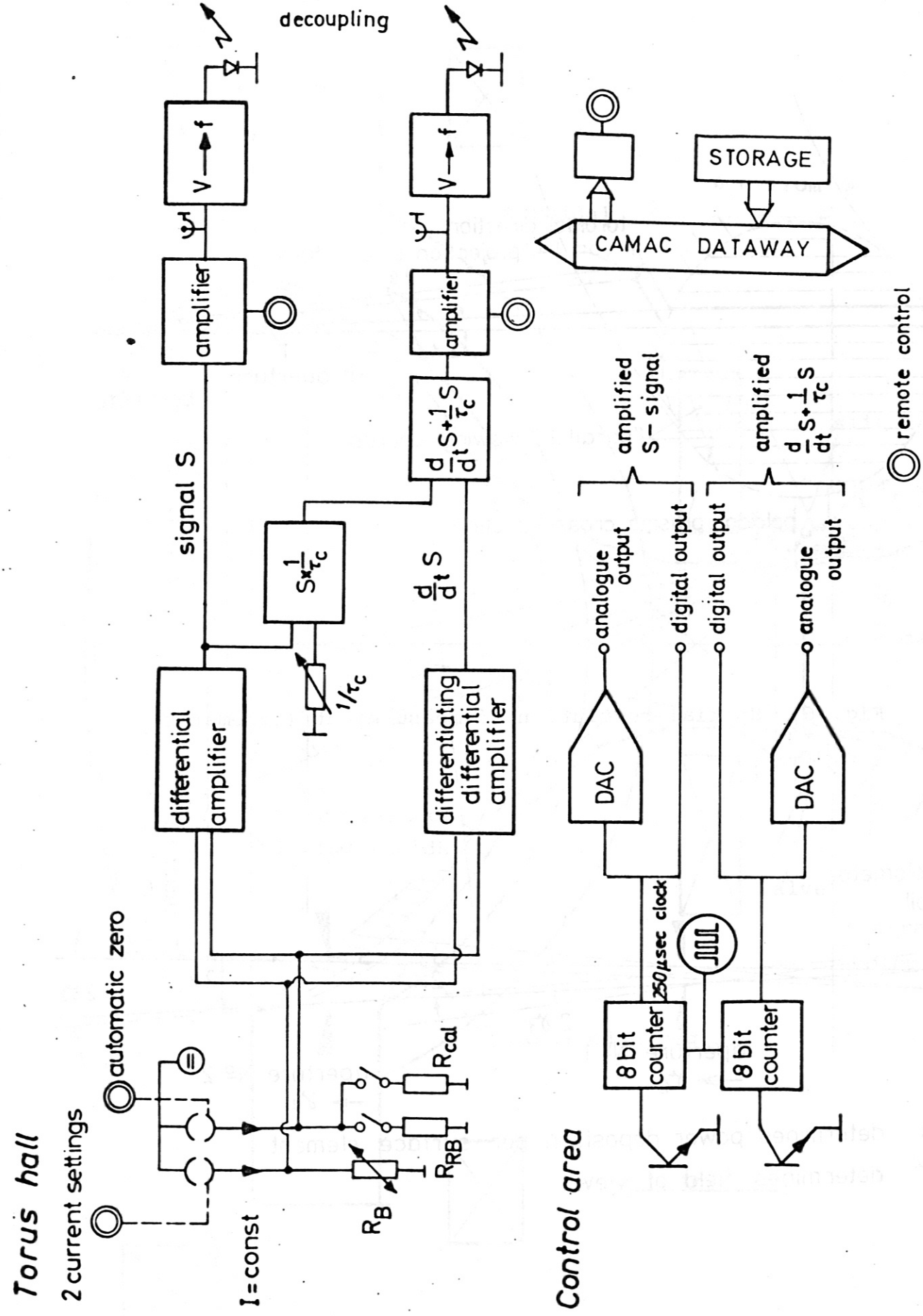

Fig. 5 Bolometer electronics for JET

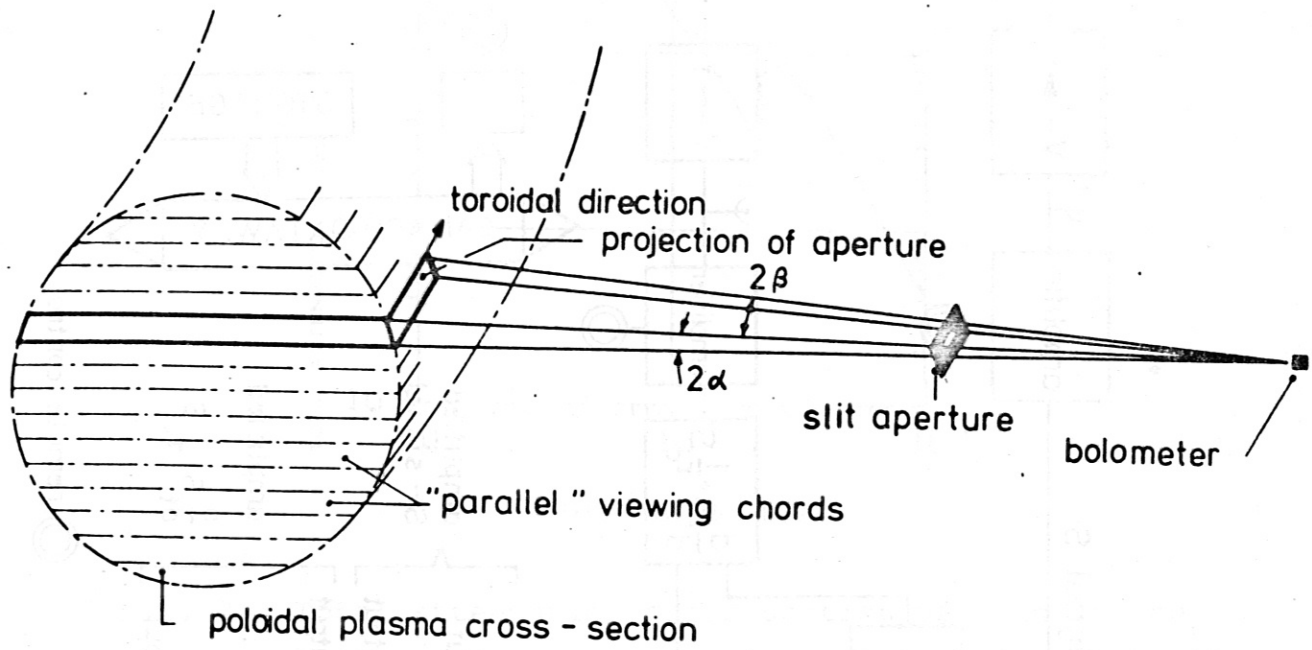

Fig. 6 Spatial resolution of measurement (schematic)

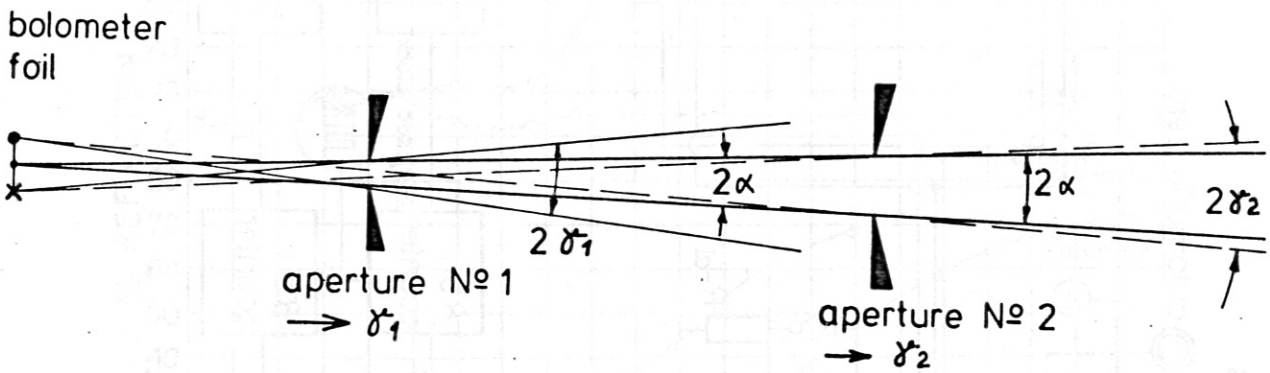

α determines power deposition per surface element

γ determines field of view

Fig. 7 Effect of not infinitely small bolometer surface

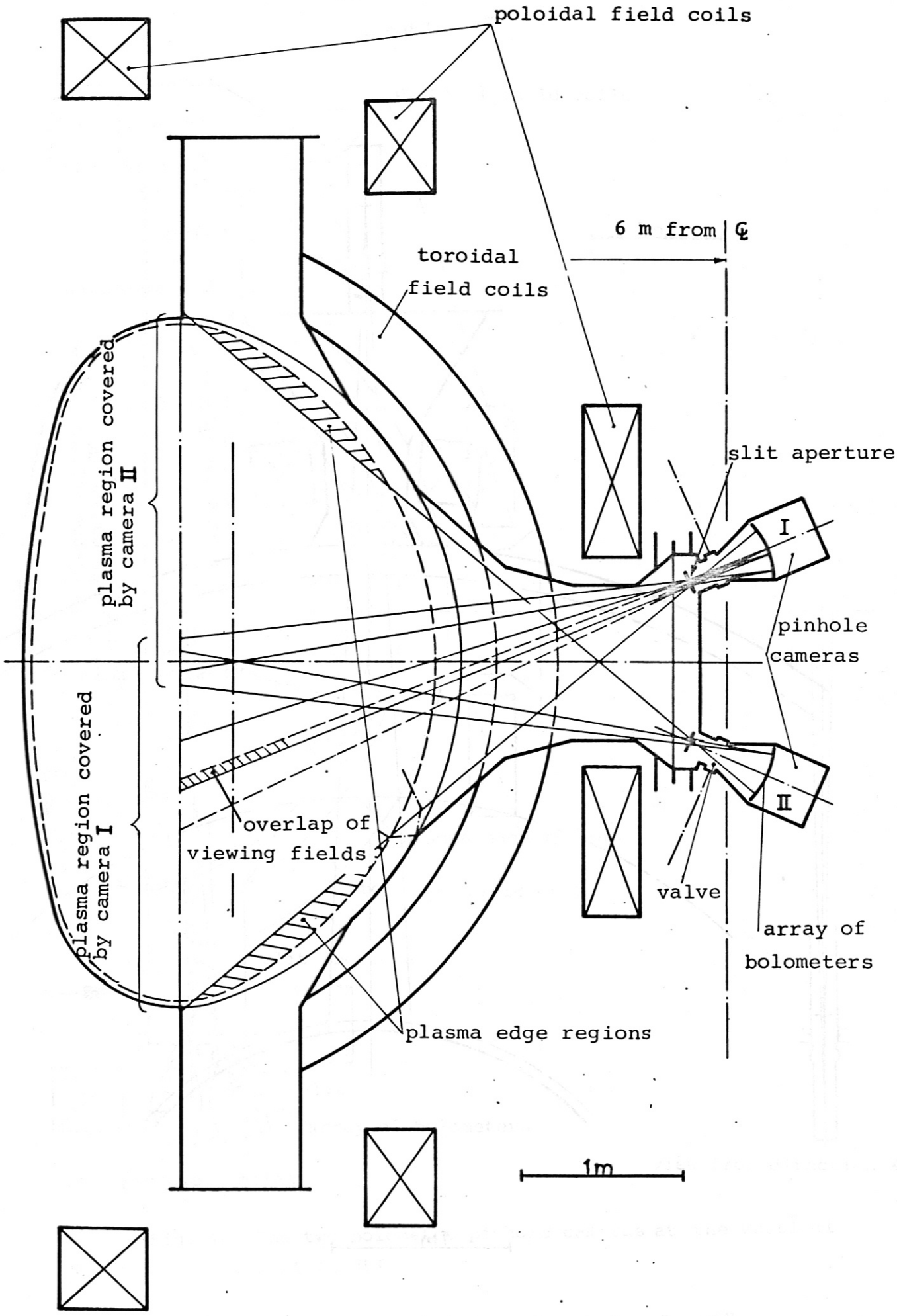

Fig. 8 The two bolometer pinhole cameras at the horizontal port of JET (poloidal cross-section)

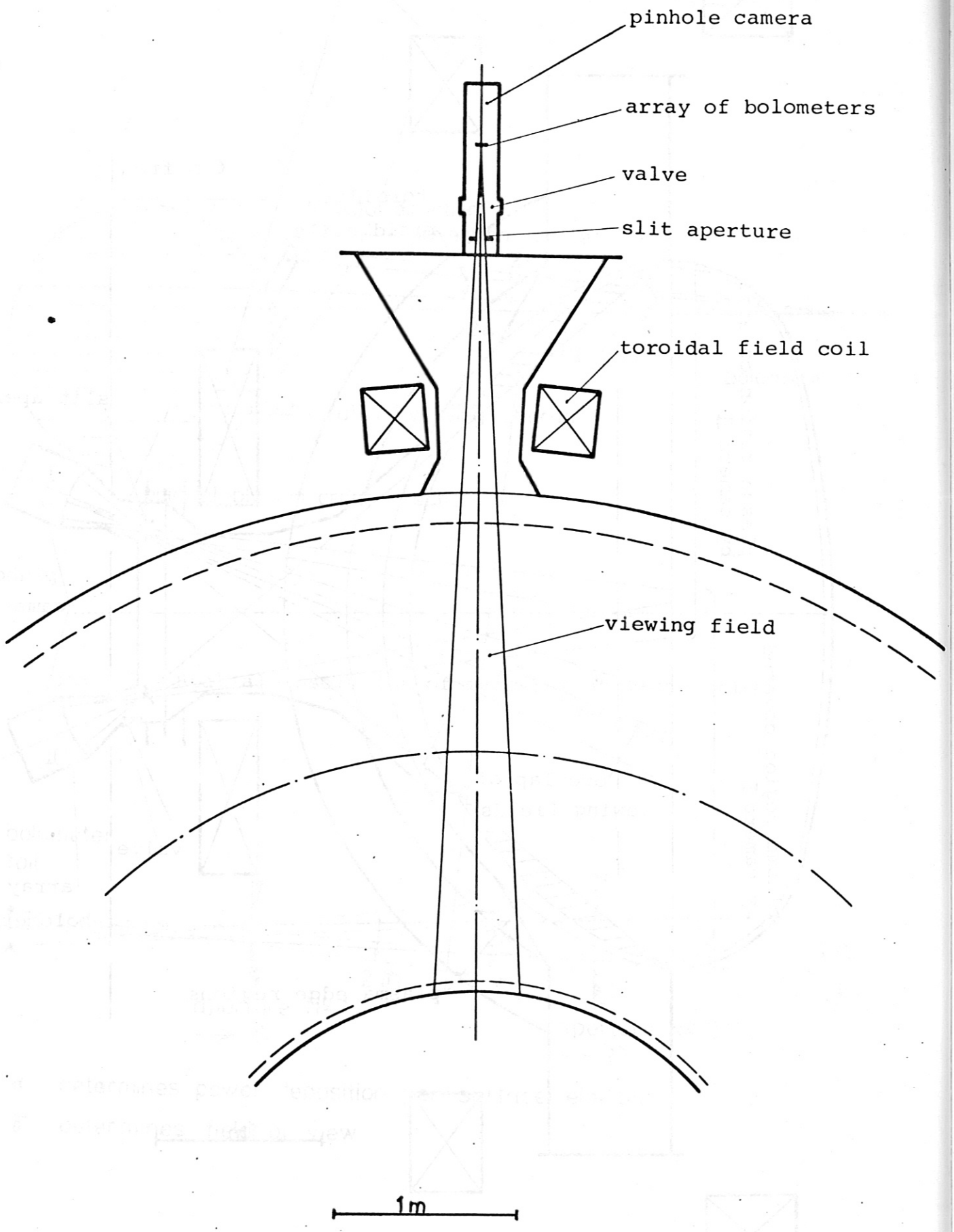

Fig. 9 Bolometer pinhole camera at the horizontal port of JET (toroidal cross-section)

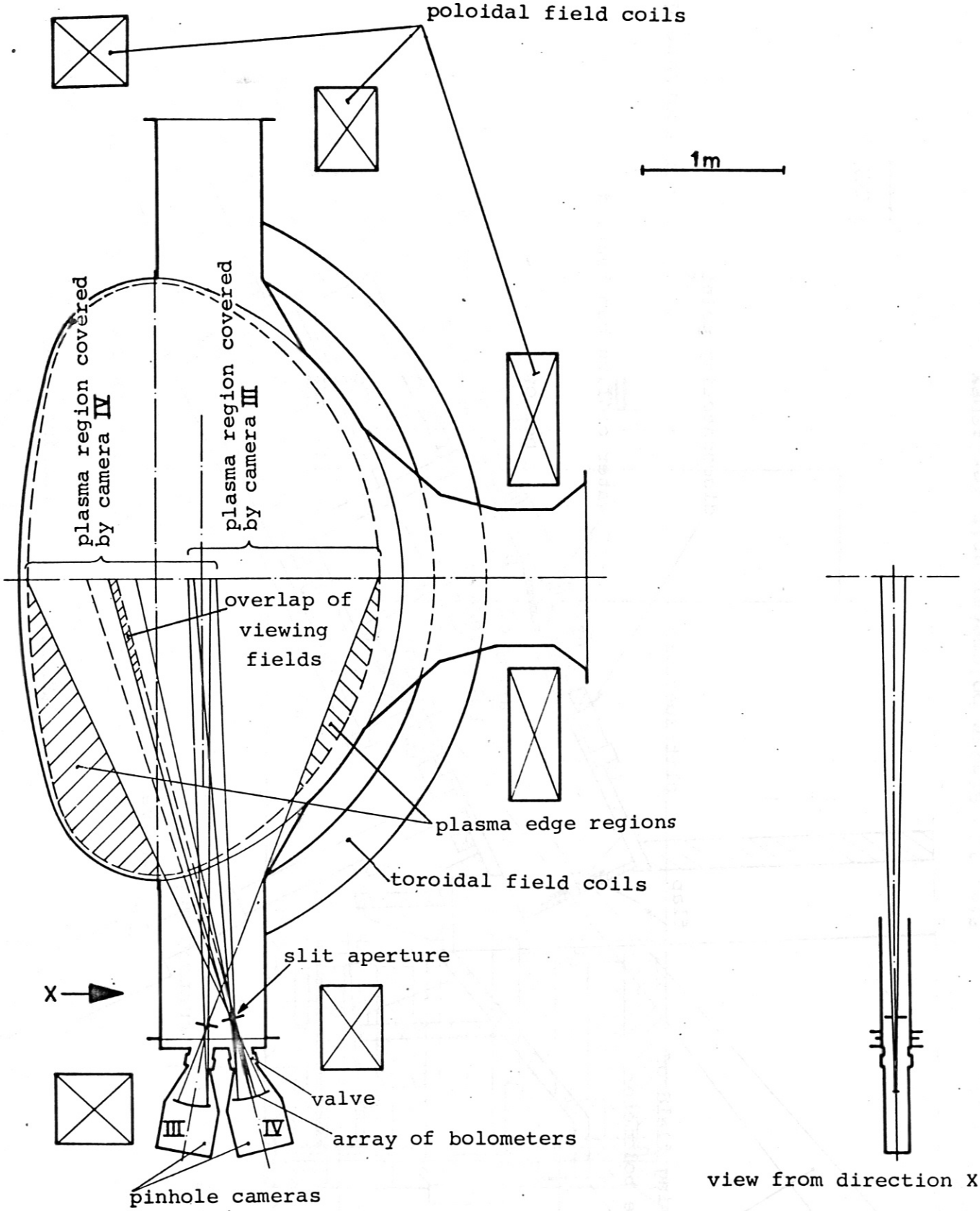

Fig. 10 The two bolometer pinhole cameras at the vertical port of JET

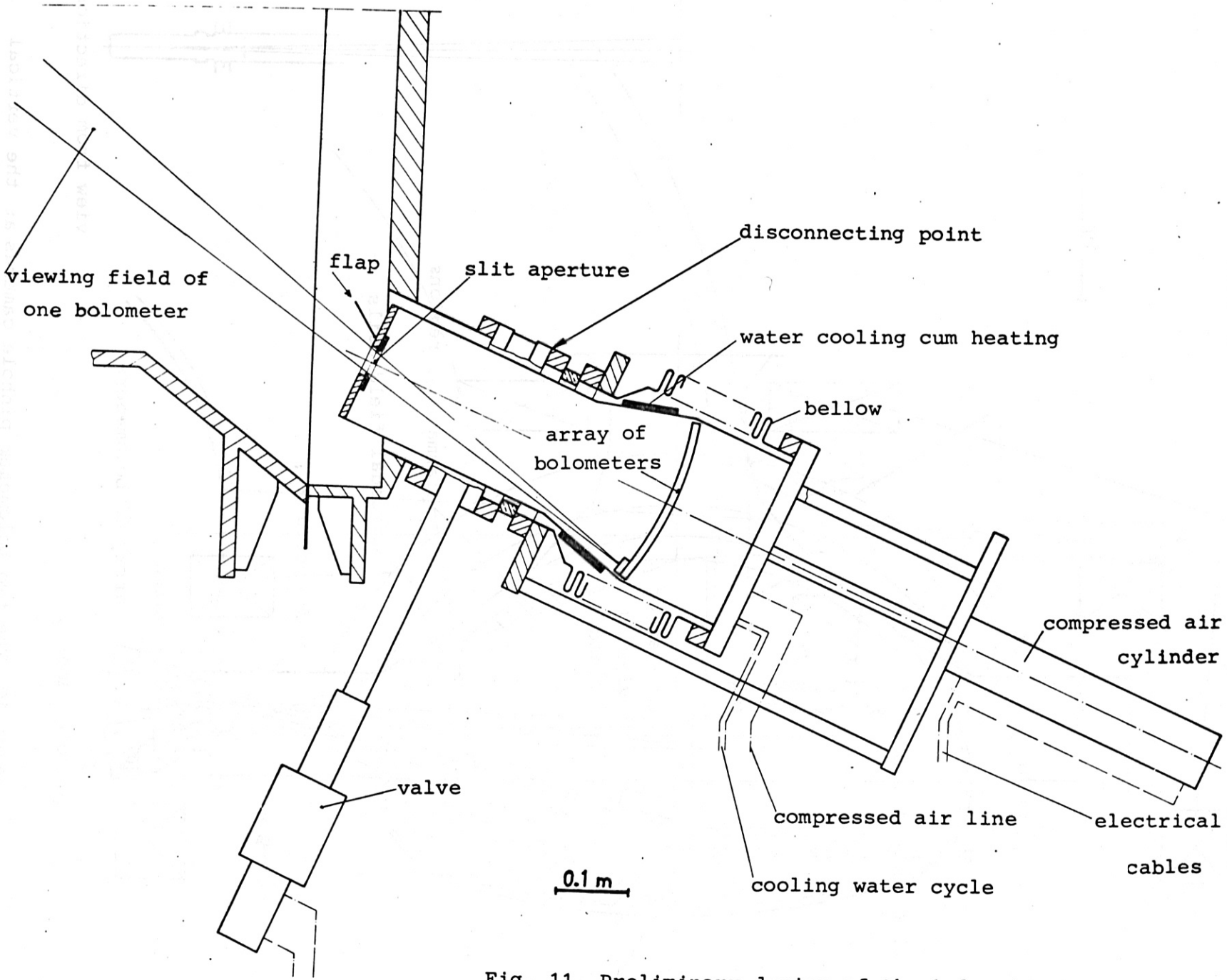

Fig. 11 Preliminary design of the bolometer pinhole camera at the horizontal port of JET

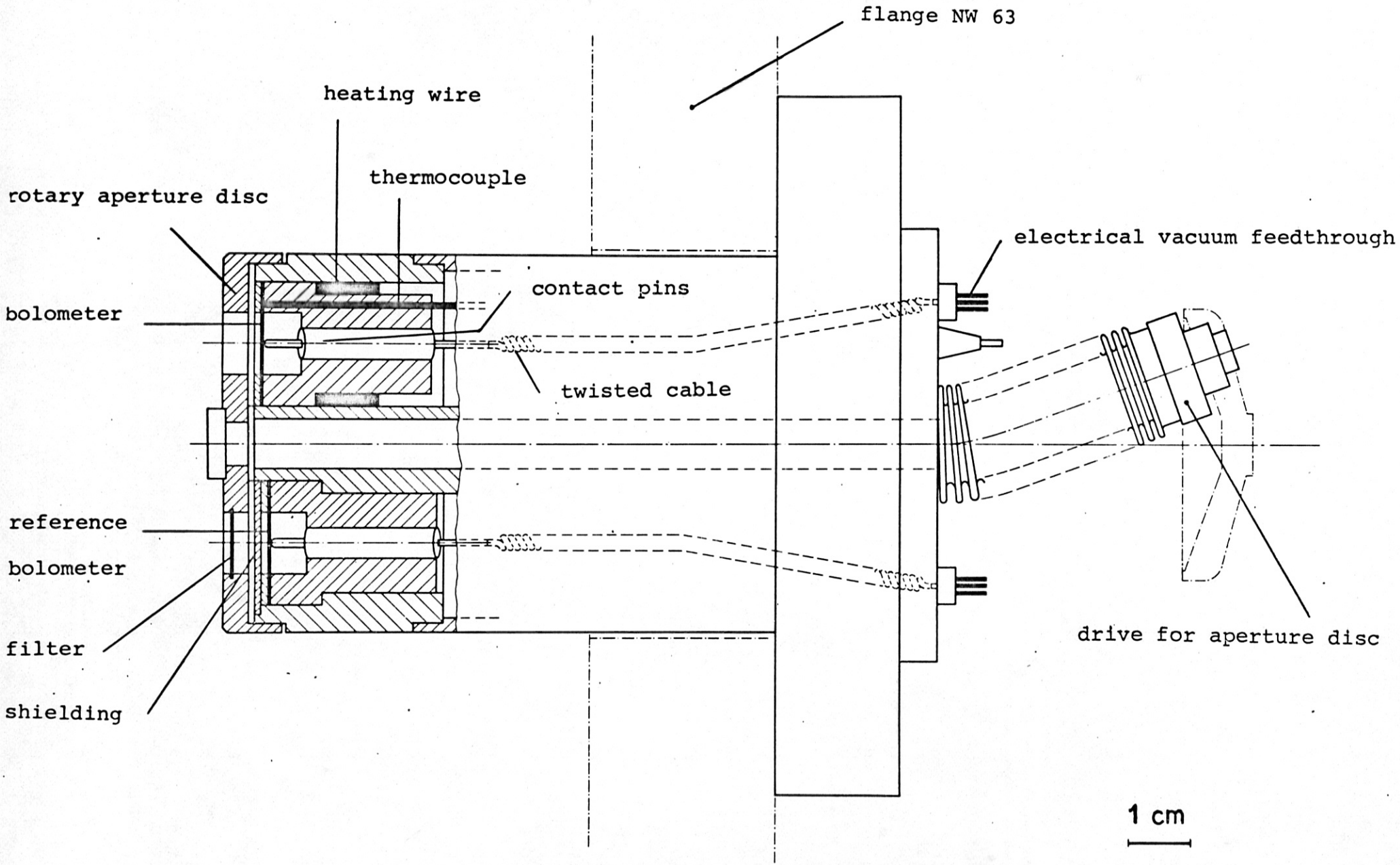

Fig. 12 Single bolometer unit for ASDEX